A Review of The Metastable Omega Phase in Beta Titanium Alloys: The Phase Transformation Mechanisms and Its Effect on Mechanical Properties

JoAnn Ballor[1, 2], Tong Li[3], Frédéric Prima[4], Carl J. Boehlert[1], Arun Devaraj[2*]
[1]Material science and engineering, Michigan State University, East Lansing, MI, 48824
[2]Physical and computational Sciences Directorate, Pacific Northwest National Laboratory, Richland, WA, 99352
[3]Institute for Materials & Zentrum für Grenzflächendominierte Höchstleistungswerkstoffe (ZGH), Ruhr-Universität Bochum, Bochum, 44801, Germany
[4]PSL Research University, Chimie ParisTech-CNRS, Institut de Recherche de Chimie, Paris, 75005 PARIS, France.
*Corresponding author: arun.devaraj@pnnl.gov

Abstract:

Since its discovery in 1954, the omega (ω) phase in titanium and its alloys has attracted substantial attention from researchers. The β-to-ω and ω-to-α phase transformations are central to β-titanium alloy design, but the transformation mechanisms have been a subject of debate. With new generations of aberration-corrected transmission electron microscopy and atom probe tomography, both the spatial resolution and compositional sensitivity of phase transformation analysis have been rapidly improving. This review provides a detailed assessment of the new understanding gained and related debates in this field enabled by advanced characterization methods. Specifically, new insights into the possibility of a coupled diffusional-displacive component in the β-to-ω transformation and key nucleation driving forces for the ω-assisted α phase formation are discussed. Additionally, the influence of ω phase on the mechanical properties of β-titanium alloys is also reviewed. Finally, a perspective on open questions and future direction for research is discussed.

Keywords: metastable omega phase titanium alloys

Table of contents

1. Introduction

Titanium (Ti) is a metal with a high strength-to-weight ratio and good corrosion resistance,[1] making it a useful material for a wide range of applications in diverse industries. β titanium (β-Ti) alloys, a subset of Ti alloys, are particularly useful because they display a wide range of microstructures and mechanical properties. The high strengths attainable by β-Ti alloys allow them to be used in critical applications, such as the use of the Ti-5553 alloy in the landing gear of the Boeing 777.[2–5] β-Ti alloys can also be tuned to have a low elastic modulus for biomedical applications because the low modulus prevents stress-shielding of the bone and decreases the likelihood of implant failures.[6,7] Thus, β-Ti alloys are widely adopted in both high-strength structural applications and lower-strength biomedical applications because their mechanical properties can be tuned to meet the needs of specific applications through judicious control of phase transformations.

β-Ti alloys contain alloying elements that stabilize the body-centered-cubic (bcc) β phase at room temperature (RT) by destabilizing the hexagonal close-packed (hcp) α phase, which is stable at RT in the case of pure Ti. These elements are called β-stabilizers, and, along with lowering the β transus temperature, they cause the Ti-alloy phase diagram to be either the isomorphous or the eutectoid-type.[1,3,8] Vanadium (V), molybdenum (Mo), niobium (Nb), tantalum (Ta), hafnium (Hf), and rhenium (Re) are β-isomorphous stabilizers, and chromium (Cr), manganese (Mn), iron (Fe), cobalt (Co), nickel (Ni), copper (Cu), and tungsten (W) are β-eutectoid stabilizers. Two examples—the isomorphous Ti-Mo and the eutectoid Ti-Cr phase diagrams—are shown in Figure 1. Additionally, aluminum (Al), oxygen (O), nitrogen (N), and carbon (C) are α stabilizers, and tin (Sn) and zirconium (Zr) are neutral to both α and β phases.

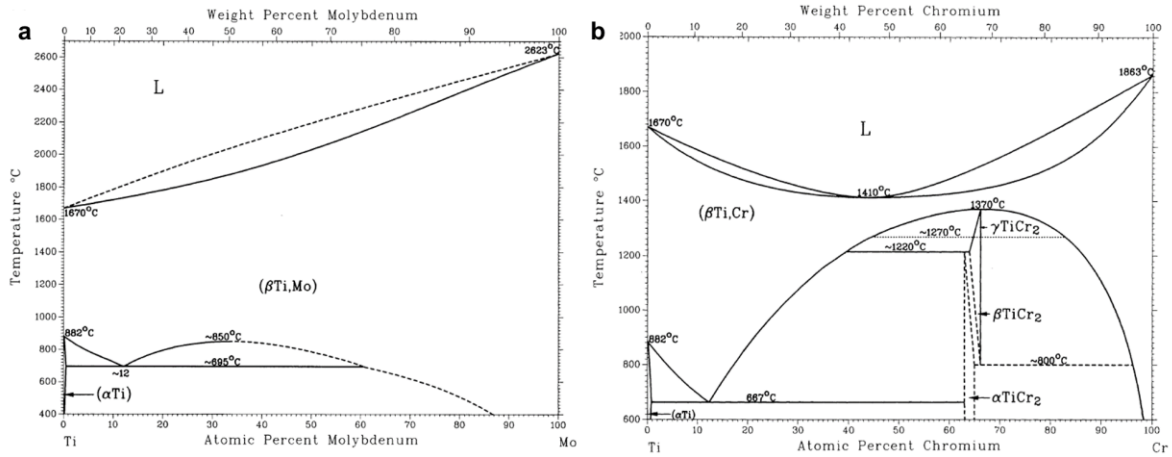

Figure 1. Phase diagrams of (a) an isomorphous-type Ti-Mo alloy and (b) a eutectoid-type Ti-Cr alloy. Adopted from J. D. Cotton, R. D. Briggs, R. R. Boyer, S. Tamirisakandala, P. Russo, N. Shchetnikov and J. C. Fanning, "State of the Art in Beta Titanium Alloys for Airframe Applications," JOM, vol. 67, no. 6, pp. 1281–1303, May 2015.

Processing β-Ti alloys allows a wide variety of microstructures to be obtained through β-to-α or β-to-α'' transformations.[1] While these transformations are commonly used to improve β-alloy mechanical properties, they can be strongly influenced by another transformation that has been of significant interest to researchers: the β-to-ω transformation.

Discovered in 1954 by Frost et al.,[9] the ω phase is a hexagonal crystal structure that can exist in pure Ti and zirconium (Zr) at high pressures,[10,11] in shock-deformed polycrystalline Ta and Ta-W alloys,[12] or in β-Ti alloys.[3,13] β-Ti alloys have been used to study the ω phase, which can occur in these alloys at a pressure of 1 atm; because these alloys are thermodynamically favorable and dynamically stable at this pressure, they can be studied without the need for specialized high-pressure equipment.[13–15] As microscopy techniques have improved over time, investigations into the ω phase have become more detailed. A surge in interest in the ω phase has coincided with the use of atom probe tomography (APT) to study the composition of β-Ti alloys on the sub-nanometer scale, and recent work has seen an increase in both understanding and debate in the field.

Despite the comprehensive amount of work in this field, many questions about the ω phase still exist, and a review of the current status of research is appropriate. This work aims to provide a summary of the current knowledge of the ω phase, including current areas of debate and opportunities for further research. All alloy compositions given in this article are in weight % unless specified otherwise.

2. Crystal structure and orientation relationships

The ω phase has a hexagonal structure that can form by the collapse of a pair of (111) planes in a bcc crystal structure into a single plane.[1,13,14,16,17] This collapse occurs when linear defects of vacancies and crowdions in the <111> direction align so that the ω structure is created from the bcc structure, changing the stacking pattern of the (111) planes from ABCABC in the bcc structure to AB'AB' in the ω structure.[18,19] Because there are four <111> directions in the bcc unit cell, four variants of the ω phase can be formed.[1,20,21] The ω phase has three atoms in the primitive unit cell and the lattice points are (0,0,0), (2/3,1/3,1/2), and (1/3,2/3,1/2), belonging to the space group $D1/6_h$, P6/mmm.[10,16] The stacking sequence is ABAB, but the ω phase is not close-packed.[14] Figure 3 shows the bcc (β phase), hcp (α phase), and hexagonal ω phase structures. The crystallographic orientation between the β, α, and ω phases has been determined as:

$$(\bar{1}\,0\,1\,0)_\omega \,||\, (1\,0\,\bar{1}\,0)_\alpha \,||\, (2\,1\,1)_\beta \quad <0\,0\,0\,1>_\omega \,||\, <1\,1\,\bar{2}\,0>_\alpha \,||\, <111>_\beta$$

$$<1\,\bar{2}\,1\,0>_\omega \,||\, <0\,0\,0\,1>_\alpha \,||\, <0\,1\,1>_\beta \quad (0\,0\,0\,1)_\omega \,||\, (\bar{1}\,2\,\bar{1}\,0)_\alpha \,||\, (1\,1\,1)_\beta$$

$$(\bar{1}\,\bar{1}\,2\,0)_\omega \,||\, (0\,0\,0\,1)_\alpha \,||\, (0\,\bar{1}\,1)_\beta$$

These relationships have been verified through multiple independent studies.[1,12,20,22–37] A representation of the $(-1010)_\omega||(211)_\beta$ relationship is shown in Figure 2.

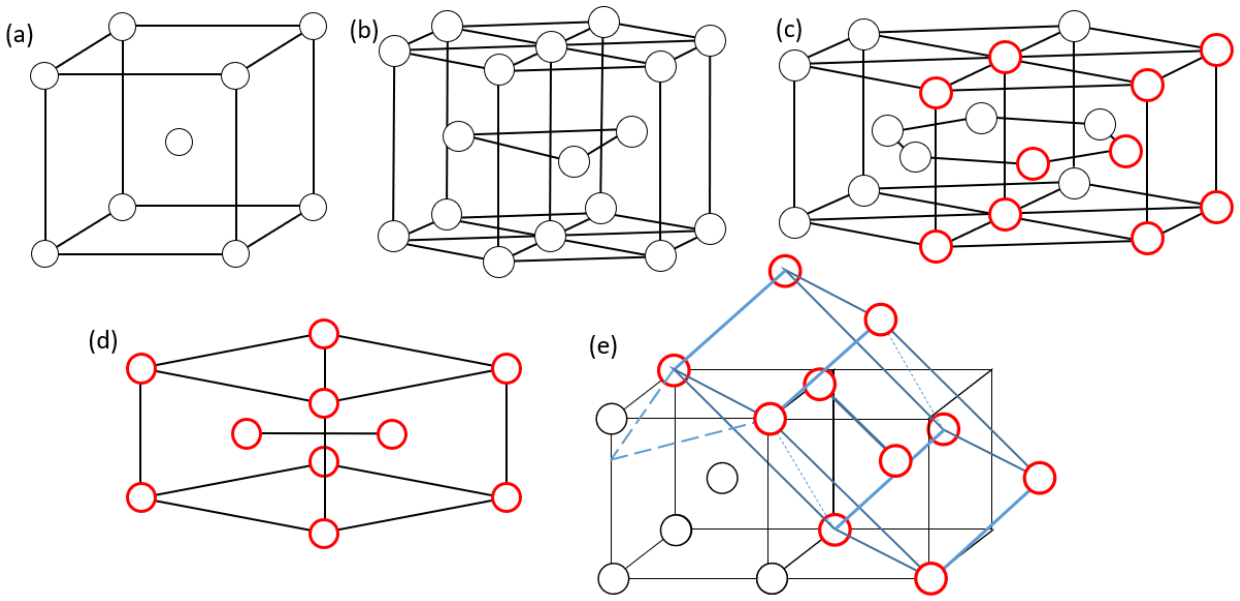

Figure 2. The (a) bcc β phase, (b) hcp α phase, (c) hexagonal ω phase with the primitive unit cell highlighted in red, (d) ω phase primitive unit cell with corresponding highlighted atoms, and (e) relationship between the β and ω phase unit cells, with the primitive ω unit cell in blue.

The ω phase in a Ti16V alloy was reported to have a lattice parameter 'a' value of 460pm and a 'c' value of 282pm.[13,16] Calculating the c/a ratio from these parameters gives a value of 0.613 and a calculated atomic packing factor (APF) of 0.68. The ω-phase APF was calculated assuming the radii of each atom in the unit cell was equivalent. In the case of the α phase, an 'a' value of 295pm, a 'c' value of 468pm, a c/a ratio of 1.588, and an APF of 0.74 has been reported.[8] Even though the reported ω phase lattice parameters are for Ti-16V and Aurelio and Guillermet[38] and Bönisch et al.[39] found that ω phase lattice parameters change with alloy content, the c/a ratio is consistently 0.613.[13,38] In Zr alloys, however, Hatt and Roberts found that the ω phase c/a ratio was 0.622,[34] and a shock-induced ω phase in polycrystalline Ta had a c/a ratio of 0.611.[12]

The ω phase APF calculation illustrates that if the plane collapse in the β-to-ω transformation occurred in pure Ti, the overall volume of the material should not change because the APF for the β phase is also 0.68.[1] The APF also helps clarify that even though the ω phase is sometimes misidentified in the literature as hcp,[8,35,40] it is not close-packed.

Selected area electron diffraction (SAED) patterns are commonly used to analyze the presence of the ω phase. ω phase diffraction spots can be imaged along the $[110]_\beta$ or $[113]_\beta$ zone axes, appearing at the $1/3<112>_\beta$ or $2/3<112>_\beta$ positions. Figure 3 shows an example diffraction pattern of the β and ω phases. These patterns have allowed the crystallographic relationships between the β and ω phases (detailed above) to be verified, such as the $(1010)_\omega$ planes having a d-spacing of 3 times that of the $(121)_\beta$ planes. These patterns have also allowed the morphology of the ω phase to be studied using dark-field imaging. Two morphologies of the ω phase—ellipsoidal and cuboidal—are observed in Ti alloys (see Figure 3).[18,41,42] The morphology of the ω phase depends on alloying elements and processing and is covered in more detail in Section 3.3.

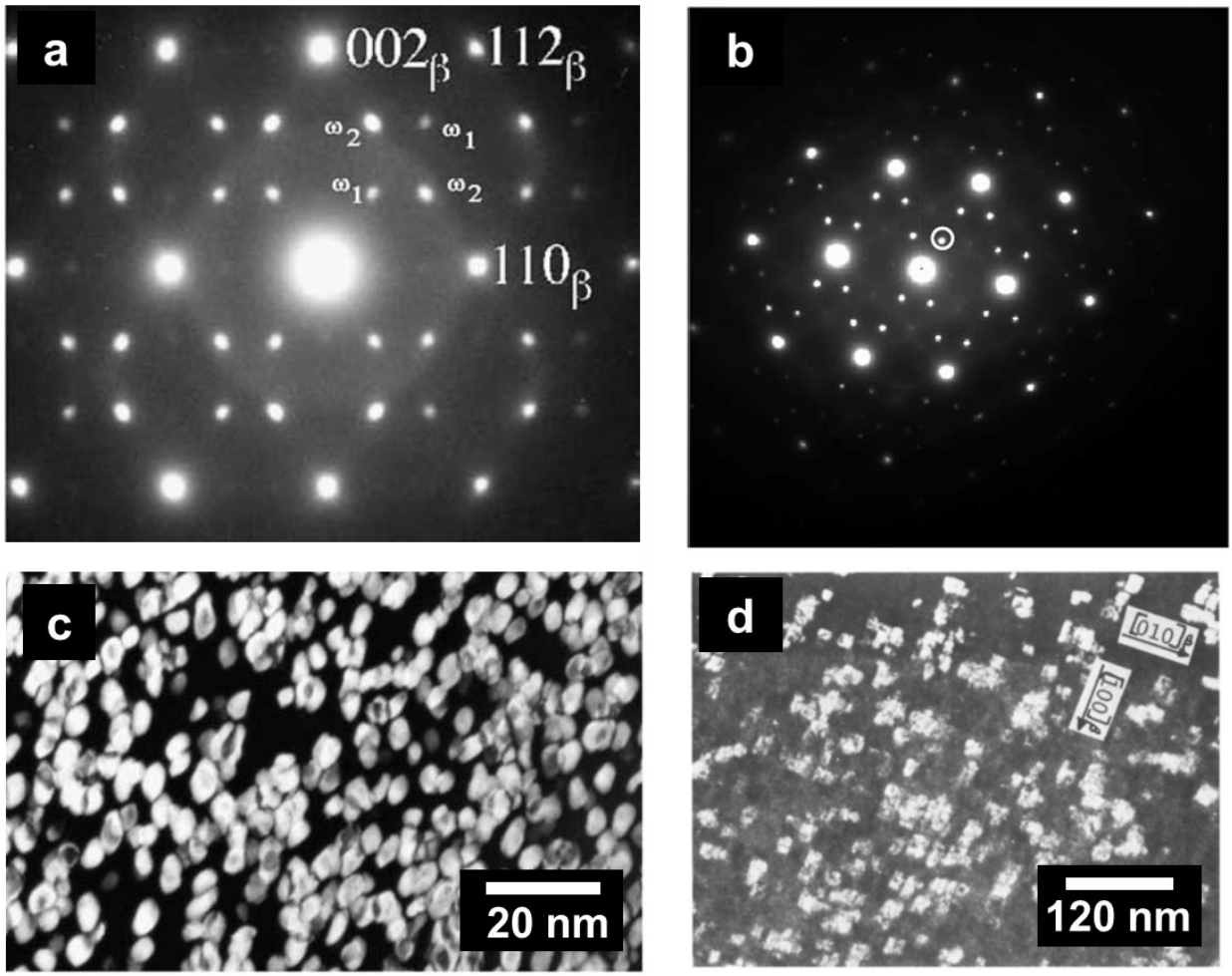

Figure 3. Examples of SAED patterns containing the β and ω phases taken from the (a) $[110]_\beta$ and (b) $[113]_\beta$ zone axes, as well as dark-field images obtained using the ω reflections in SAED patterns showing the (c) ellipsoidal and (d) cuboidal morphologies of the ω phase. ((a, c) adapted from F. Prima et. al., *Scripta Materialia,* vol. 54, pp. 645–648, 2006. (b) from J. I. Qazi et. al., *Materials Science and Engineering C,* vol. 25, pp. 389–397, 2005. (d) from V. Chandrasekaran et. al. *Metallography,* vol. 11, pp. 183–198, 1978).

3. Classification of ω phases

The plane collapse that creates the ω phase in β-Ti alloys is initiated by one of three mechanisms: pressure/plastic deformation, quenching from above the β-transus, or thermal energy. Compositional differences in the β phase can facilitate these mechanisms,[20,43,44] which create different types of the ω phase. While these types have the same crystal structure (outlined above), they are differentiated in the literature to help the reader distinguish between the formation mechanisms. These distinctions are useful because the formation mechanism can affect the size, morphology, and composition of the ω phase. The generally recognized types of ω phase are the (1) **deformation-induced ω phase,** (2) **athermal ω phase (ω_{ath}),** and (3) **isothermal ω phase (ω_{iso})**. A detailed analysis of the state of the knowledge of each type of ω phase is given below.

3.1 **Deformation-induced ω phase**

The deformation-induced ω phase can be studied in pure Ti and Zr through the application of high static pressures because the structure remains stable after the pressure is removed.[10,11,45–48] This is true of β-Ti alloys as well as pure α-Ti. β-Ti alloys have four stress-induced transformations: the α' and α'' martensites, the ω phase, and mechanical twins.[17] Low concentrations of β-stabilizing elements favor α'- and α''-martensitic transformations (decreasing the M_S temperature). Higher concentrations of β-stabilizing elements suppress the α' and α'' transformations, allowing the ω phase and twins to form instead,[17,49] with the ω phase forming in both the β matrix and inside of the twins.[49,50] If a β-stabilizer concentration is reached that is high enough, the ω-phase transformation will also be suppressed and only twins will form.[17,51] Clear cutoffs for low, medium, and high β-stabilizer concentrations are not well defined in the deformation-induced ω-phase literature. Comparing β stability between studies of the deformation-induced ω phase can be difficult because different alloys are often used, such as Xing and Sun's Ti-23Nb-0.7Ta-2Zr-0.2O (at%) alloy[52] and Ahmed et al.'s Ti-10V-3Fe-3Al alloy.[50]

One way to compare alloys between studies is through the Mo Equivalency (Mo-Eq) equation.[8,53] Mo-Eq is a way to compare different β-Ti alloys with different alloying elements and concentrations by finding the equivalent concentration of molybdenum that, if alloyed instead, would provide an equivalent amount of β stability. This is done by dividing 10 wt.% Mo by the minimum wt.% of each stabilizing element needed to create a completely β-stable alloy (where 100% of the β phase is retained upon quenching from above the β transus) and multiplying the division with the wt.% of each stabilizing element, then summing the results.[53] This gives the Mo-Eq equation:

$$Mo\ -Eq = Mo + 0.67 * V + 0.44 * W + 0.28 * Nb + 0.22 * Ta + 2.9 * Fe + 1.6 * Cr - 1.0 * Al$$

where the elemental symbol is the amount of that element in weight percent.[53] While not a perfect way to compare β-Ti alloys because some of the elements are isomorphous stabilizers and some are eutectoid stabilizers, Mo-Eq provides a reference point for comparison. Even using Mo-Eq, it is still difficult to compare β stability between alloys.

In general, a low β-stabilizer concentration seems to refer to alloys with a Mo-Eq of less than 10.[54] The β phase stability range where the ω phase forms is a Mo-Eq of approximately 10–12.5.[50–52,54,55] A range of ~12 to 15 supports deformation-induced twin formation, with or without the ω phase.[55,56] A Mo-Eq higher than ~15 supports slip as the dominant deformation mechanism.[54] These ranges are only general guidelines for β-Ti alloys and exceptions to these ranges can be found, such as twins and ω phase forming along with α'' martensite in a cold-rolled Ti-24Nb-4Zr-8Sn alloy (Mo-Eq of ~6.7)[49] and ω phase forming in a Ti-3Nb (Mo-Eq of 0.86) alloy after high-pressure torsion (HPT).[57]

However, β-stabilizer concentration is not the only variable that affects deformation-induced ω phase formation. Grain size,[26] processing route,[50] and the existence of deformation twins[48] have been shown to affect the volume fraction of the ω phase. In static-pressure experiments, impurities such as O or N increased the pressure required to initiate deformation-induced ω phase formation.[45]

Severe shear plastic deformation during HPT has been shown to induce formation of the ω phase in Ti and its alloys. The torsion that the samples experience lowers the incubation time for ω phase formation in Ti by approximately 27 hours compared to static pressure alone[58] and reduces the amount of pressure needed to generate the ω phase.[59] β-stabilizer concentration affects the amount of ω phase in the material after HPT processing.[60,61] Annealing temperature before HPT processing can also affect the volume fraction of the ω phase formed.[57] However, Tane et al.[62] and Panigrahi et al.[63] demonstrated that HPT processing can lead to the formation of a deformation-induced ω phase in pure Ti and Ti-16.1Nb alloys. The starting microstructure can affect the number of turns needed to start the ω phase

transformation[60] as well as the amount of ω phase in the material formed after HPT.[64] HPT can also induce an α-to-ω phase transformation[58,64] through atomic shuffles in the $(0001)_\alpha$ planes.[60] However, the α-to-ω transformation is not guaranteed to form in all Ti alloys during HPT.[64] Wang et al.[26] and Edalati and Horita[65] found that grain size is an important variable that influences the ω-phase formation in both β-Ti and pure Ti, with smaller grains lowering the amount of ω phase in the material, although temperature was also a variable in the Edalati and Horita study.[65]

Multiple morphologies are reported for the deformation-induced ω phase. In compression testing, long, thin lamellar ω phases were generated.[50] During hot deformation in the β + α region, a thin lamellar-like ω phase was also reported to form.[35] Impact testing formed a plate-like ω phase.[66,67] Cold-rolling also produced plate-like ω phase.[49] In polycrystalline Ta and Ta-W alloys, the shock-generated ω phase had a zigzag structure with multiple interconnected ω-phase variants.[12] Also, alloying Ta with the β-stabilizer W increased both the volume fraction and the size of the ω phase.[12]

3.2 **Athermal ω phase**

The athermal ω phase forms as well-dispersed particles during the quenching of β-Ti alloys from above the β transus temperature when the $(111)_\beta$ plane collapse occurs as a result of the instability of the β phase with respect to a specific mode of phonon.[21,68,69] ω_{ath} particles are less than 10 nm in size—usually between ~2 and 5 nm[1,20,28,49,70–72]—and are generally reported as spheroidal[20,35,50,71,73] or ellipsoidal.[28,35,70,72] Because quenching does not allow diffusion to occur, ω_{ath} theoretically has the same composition as the surrounding β matrix,[74] with higher volume fractions forming in β alloys with β stabilizer concentrations close to the lower limit of β-phase retention.[13,31,75]

As a result of the small size of ω_{ath}, local strain fields around ω_{ath}, and/or short-range correlated displacements in the β lattice, ω_{ath} is observed to lead to diffuse streaking in SAED patterns rather than discrete diffraction spots.[34,68,69,76,77] Diffuse streaking in selected area diffraction patterns are also observed when there is an incomplete collapse of the $(111)_\beta$ planes during the β-to-ω transformation. Instead of being located at (0,0,0), (1/3,2/3,1/2), and (2/3,1/3,1/2), the atoms have positions at (0,0,0), (1/3,2/3,1/2+δ), and (2/3,1/3,1/2-δ), where $0<\delta<1/6$. The value of δ depends on the degree of plane collapse, with smaller δ values corresponding to lower β-stabilizer concentrations.[14,78] Although the existence of the partially collapsed ω phase has been debated,[68] high-resolution STEM (HRSTEM) images have definitively proved its existence.[20,25,43] Sometimes referred to as "rumpled" ω,[12] "rumpled-plane" ω,[34] trigonal ω,[14] "modulated" ω,[79] or "embryonic" ω,[20,25,27,80] these "incommensurate" structures have also been reported with the fully collapsed "commensurate" ω_{ath} after quenching.[20,69,76,78] However, it is important to note that these ω structures can also form during heat treatments, causing diffuse streaking in selected area diffraction patterns of quenched and isothermally aged samples.[27,81] Figure 4 shows an example of the incommensurate ω phase as seen in high resolution transmission electron microscopy (HRTEM), along with graphical representations of the incommensurate and commensurate ω structures.

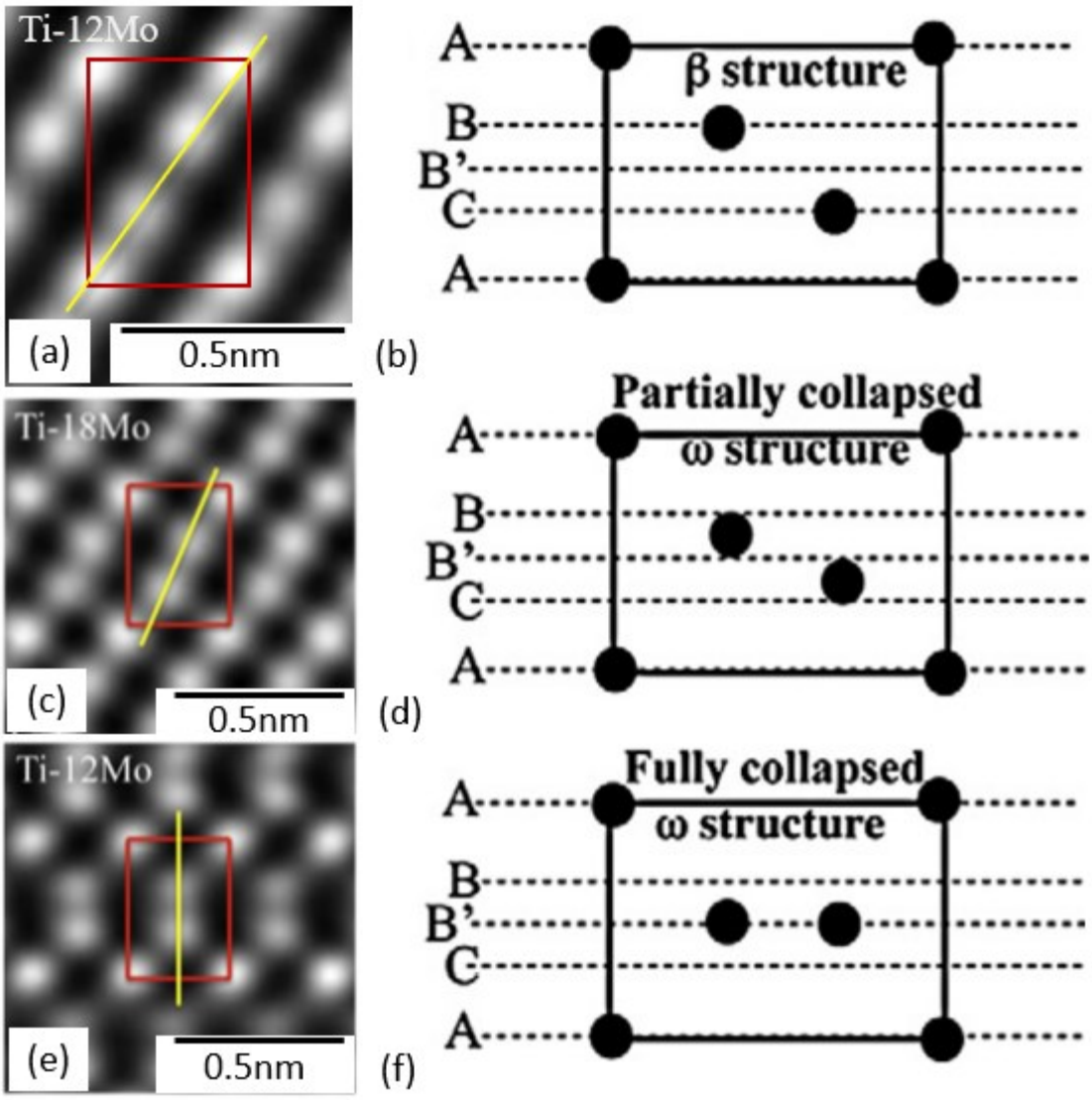

Figure 4. (a) An HRTEM image and (b) a schematic of the β structure, (c) an HRTEM image and (d) a schematic of the partially collapsed "incommensurate" ω structure, and (e) an HRTEM image and (f) a schematic of the fully collapsed "commensurate" ω structure in Ti-Mo alloys. (All HRTEM images adopted from Zheng, Y., Banerjee, D., and Fraser, H.L. *Scripta Materialia*, V. 116, 2016, pp. 133. All schematics adopted from Devaraj et al. *Acta Materialia,* V. 60, No. 2, 2012, pp. 604).

The different types of ω phase (deformation-induced, athermal, and isothermal) are differentiated via their formation pathway (deformation, quenching, heat treatment). Because the incommensurate ω phase can form through either quenching or heat treatment, labeling it as solely an athermal or isothermal type of ω phase is not sufficient and the literature to date has been inconsistent with its nomenclature. Therefore, in the remainder of this article, the authors use the terminology "athermal ω phase" or "ω_{ath}" to mean a commensurate ω phase that forms through quenching and "isothermal ω phase" or "ω_{iso}" to mean a commensurate ω phase that forms during isothermal aging. To refer to incommensurate ω phase formed through the athermal pathway, "incommensurate athermal ω phase" or "incommensurate ω_{ath}" is used. Similarly, "incommensurate isothermal ω phase" or

"incommensurate ω_{iso}" is used to refer to incommensurate ω phase formed through the isothermal pathway.

3.3 **Isothermal ω phase**

The isothermal ω phase precipitates homogeneously in metastable β-Ti alloys during low-temperature heat treatments that favor the β-to-ω transformation over the β-to-α transformation.[8,13,69,82–85] Depending on the alloy, the lowest temperature that initiates the β-to-ω_{iso} transformation is between 150 °C[24] and 280 °C.[86] Most researchers use a temperature range of 300 °C–400 °C to generate the isothermal ω phase,[23–25,27,30,32,33,41,80,86–88] and 500°C is the highest temperature reported to form ω_{iso}.[39,89] Using in situ synchrotron diffraction experiments, Bönisch et al.[39] found that the ω phase lattice parameters remained relatively constant in both Ti-28.5Nb and Ti-36Nb as they were heated from 300 °C to 500 °C.

ω_{iso} has been found to nucleate at defects in the β matrix left by ω_{ath} after ω_{ath} reverts to β phase during heat treatment.[24,90] ω_{iso} has also been found to grow from $\omega_{ath.}$[21,22,74] Locations in the β matrix with lower concentrations of β-stabilizers due to nanoscale chemical fluctuations are also favorable sites for ω_{iso} nucleation.[20,25,43] Because of the relationship between ω_{ath} and ω_{iso}, Prima et al. have proposed that the volume fraction of ω_{iso} formed in the β phase can be indirectly controlled using ω_{ath}.[90] ω_{iso} nucleation is also influenced by aging temperature, as Prima et al. had a higher volume fraction of ω_{iso} form after aging at 310 °C than at 250 °C.[24]

During the growth of ω_{iso} particles, alloying elements diffuse from the ω phase into the surrounding β matrix.[1,13,14,86,91] APT is a powerful technique for investigating sub-nanometer scale, spatially resolved composition of precipitate phases,[92] and APT studies of multiple binary β Ti alloys clearly show that the ω phase is solute-lean (shown in Figure 5).[20,32,43,70,93] For example, in a binary Ti-9.9Mo (at%) alloy, the ellipsoidal ω phase was found to have a Mo concentration near 2 atomic %.[20,93] More complex alloys have also been studied using APT, showing that ω_{iso} is depleted of both β- and α-stabilizing elements.[22,27,30,71,80,82,83,87,94,95]

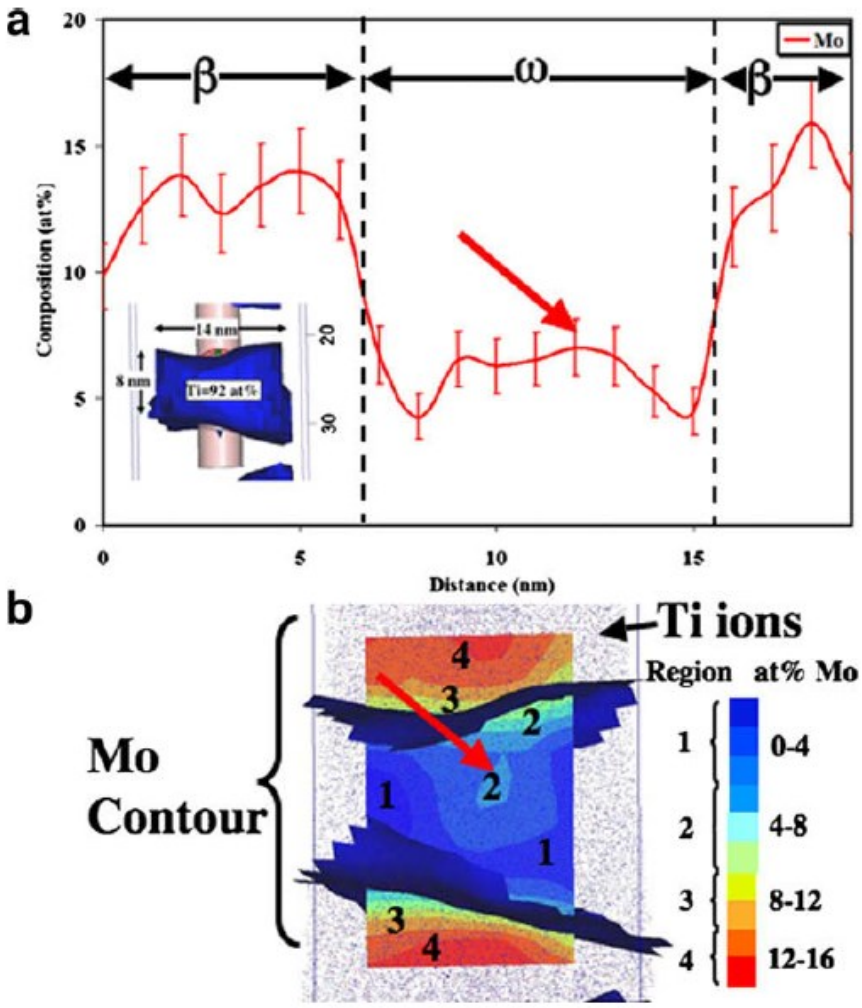

Figure 5. (a) A Mo composition plot taken from a 1-D cylinder showing the Mo composition difference between the β matrix and an ω-phase particle and (b) the associated Mo contour plot. (Figure adopted from A. Devaraj, et al., "Three-dimensional morphology and composition of ω precipitates in a binary titanium-molybdenum alloy," *Scripta Materialia,* vol. 61, pp. 701–704, June 2009).

The size of ω_{iso} particles depends on the time spent at the heat treatment temperature because the particles coarsen with time. A range of 2–100 nm has been reported for ω_{iso} particles generated using various temperatures and times.[20,23,25,28,42,70,71,74,82,83,88,93,96] Moffat and Larbalestier[96] have also shown that higher aging temperatures produce larger precipitates for the same amount of time. Because of the small size of ω_{iso}, transmission electron microscopy (TEM) is the most effective microscopy technique for detecting the ω phase in materials, although some studies have detected the presence of the ω phase using X-ray diffraction.[31,89,94,97]

Heat treatment temperature and time also affects the volume fraction of ω_{iso} formed.[98,99] For example, holding a Ti-12wt% alloy at 450C for 50 hours forms a higher volume fraction of ω_{iso} than holding the same alloy at 400 °C for 250 hours.[98] The combination of temperature and time that produces the highest volume fraction of ω_{iso} also changes with alloy composition, shown by Hickman when a Ti-8Mo

(at%) alloy reaches a maximum ω_{iso} volume fraction of 0.78 after 175 hours at 350 °C while a Ti-10Mo (at%) alloy formed a maximum ω_{iso} volume fraction of 0.56 after 8 hours at 400 °C.[99]

The morphology of the ω phase is determined by the elastic strain energy in the crystal that is due to the difference between the radii of alloying elements and Ti[21,93] or by elastic interactions between the ω_{iso} particles.[100] ω_{iso} particles in high-misfit systems, such as Ti-Cr, have a cuboidal morphology with the flat surfaces parallel to the $(110)_\beta$ planes.[1,93,96] ω_{iso} particles in low-misfit systems, such as Ti-Mo, have an ellipsoidal morphology in which the major axis is parallel to the $<111>_\beta$ directions[1,36,93,96] as a result of the elastic anisotropy of the β phase, and an average ratio of the major to the minor axis of 3.56.[93] With enough time, the ellipsoidal ω_{iso} particles in low-misfit systems become cuboidal because the elastic interactions between the particles affect the morphology with increasing growth of ω_{iso}.[100] Blackburn and Williams[36] show this transformation from ellipsoidal morphology to a cuboidal morphology of ω_{iso} in a high-misfit Ti-V alloy. Figure 3 above shows dark-field TEM images of ω_{iso} particles with the two morphologies. Furthermore, for a low-misfit Ti-6554 alloy, the morphology of ω_{iso}—which grew from an ellipsoidal incommensurate isothermal ω phase—was observed to evolve from more lath-like to a mixed plate- and rod-like morphology as the annealing time increases at 300 °C.[27]

Because of the effects of ω_{iso} on mechanical properties (covered in detail below), methods have been developed to avoid precipitation of ω_{iso}. Precipitation of the isothermal ω phase can be avoided through the addition of alloying elements that increase the stability of the β phase[15,89,101] or the α phase (such as oxygen or aluminum).[29,101–103] Heat treatment temperatures above 500 °C can be used to precipitate the α phase without precipitating the ω phase,[13,69,84]. However, the ω phase might still be precipitated if the heating rate to reach temperatures above 500 °C is slow enough to allow ω precipitation or if the α'' phase was present before heating and a fast heating rate is used.[40,104,105] Increasing the amount of time the alloy stays at lower heat treatment temperatures (100 °C–500 °C) can cause the α phase to grow into the ω phase, leaving only the α crystal structure and no ω crystal structure;[23,25,27,42] in some alloys, however, ω_{iso} can coexist with α after heat treatments of 192 hours.[25,30] ω phase formation can also be suppressed by large quantities of grain boundaries or dislocations that prevent $(111)_\beta$ plane collapse.[84]

4. β to ω phase transformation mechanism

ω_{ath} and deformation-induced ω are formed through a displacive mechanism via atomic shuffling. Driven by quenching or stress, the $(111)_\beta$ plane collapse occurs without diffusion. The displacive collapse is reversible, as De Fontaine et al. showed through in situ TEM ω_{ath} formation and reversion in the temperature range of −171 °C to 5 °C, which prevented diffusion.[68] The combination of temperature increase from electron irradiation and oscillations from inelastic scattering in a TEM can also reverse the displacive collapse.[73]

In comparison, the isothermal ω phase is known to form via a diffusion mode. That is, elemental partitioning occurs along with the $(111)_\beta$ plane collapse, creating an ω phase with a lower energy than the ω phase generated through displacive collapse.[15] While the isothermal ω phase has been shown to grow rapidly without diffusion for short times (60 seconds) at the start of nucleation,[21,71,106] the rejection of the β stabilizers is important for isothermal ω phase growth because it stabilizes the ω phase by lowering the energy of the structure and making the ω transformation irreversible.[68] Quenching before the heat treatment and heating during isothermal aging are necessary to make the β-to-ω transition more energetically favorable than the β-to-α transition, with faster quenching rates increasing the number of ω_{iso} precipitates formed.[96,103,107] This is attributed to the relationship between ω_{ath} and ω_{iso} because ω_{ath}

locations in the β matrix have been shown to act as nucleation sites for ω_{iso}.[14,90] However, the exact mechanism behind ω_{ath}-assisted precipitation of ω_{iso} is not known. Additionally, a slow heating rate is found to allow nucleation and growth of ω_{iso} particles from the β phase during heating,[40,104,105] although Barriobero-Vila et al.[105] have shown that if α''martensite is present, a faster heating rate increases the volume fraction of ω_{iso} compared to slower heating rates by activating the α''-to-ω_{iso} transformation along with the β-to-ω_{iso} transformation.

Current debate about the β-to-ω transformation centers around the athermal and incommensurate ω_{iso} phases (which are early stages of ω_{iso}). Nag et al.[43] and Devaraj et al.[20] found evidence that incommensurate ω_{iso} particles formed in pockets of slight Mo-depletion in a binary Ti-Mo alloy during quenching, and Li and Min[78] found incommensurate ω_{ath} in Mo-lean regions in a Ti-15Mo alloy. Li and Min also suggest that the shear modulus is softened in the Mo-lean regions of Ti-Mo alloys, which allows the $(111)_\beta$ planes to collapse more easily.[78] These results seem to agree with predictions by Gullberg et al.[108] and earlier findings by McCabe and Sass[109] that ω_{ath} is Ti rich, as well as with observations by Fan and Miodownik[44] that the ω phase forms in solute-lean β phase areas more readily. They also support findings by Nag et al.[110] that suggested ω_{ath}/incommensurate ω phase particles were associated with fluctuations in stabilizer concentrations. More recent work by Li et al.[25,27] supports this as well, finding that the incommensurate ω_{iso} particles in Ti-6Cr-5Mo-5V-4Al were Mo lean. However, they clarified that the Mo-lean pockets were created by second-order spinodal decomposition of the β phase and that the incommensurate ω_{iso} phase forms via a displacive mechanism within these Mo-lean regions.[25] Tane et al.[111] came to a similar conclusion with their work in a Ti-V alloy system, showing that the ω phase can form without diffusion in quenched-in V-lean pockets while aging at room temperature. In contrast, Ahmed et al.[40] and Ng et al.[71] have found no change between the matrix composition and the composition of the athermal ω phase. Coakley et al.[87] also did not observe the formation of ω_{ath} in Mo-lean pockets in Ti-5Al-5Mo-5V-3Cr. Sun et al.[106] and Mantri et al.[112] both found no compositional variation in a Ti-12Mo alloy associated with the formation of ω_{ath}, but both recorded sharp diffraction spots—this suggests a lack of the incommensurate ω phase, which Nag et al.,[43] Devaraj et al.,[20] and Li et al.[27] all observed forming in the Mo-lean pockets.

5. ω-assisted precipitation of the α phase

Another important phase transformation is the ω-to-α phase transformation. ω_{iso} is known to affect the precipitation of the α and α'' phases.[21,37,84] The finely distributed α platelets formed by ω-assisted precipitation were noted by Ohmori et al.[37] to have a significantly deviated habit plane compared to the coarse α plates formed without ω-assistance. It should be clarified that ω_{ath} and the incommensurate ω_{iso} phases do not assist in α formation[27,32,113,114] but they can coexist with the α phase.[27,69] The commensurate ω_{iso} phase promotes the formation of refined α precipitates, thereby providing attractive mechanical properties for high-strength applications.[22] A fine-grained α-phase also formed in HPT samples composed of the deformation-induced ω-phase when heated above 320 °C, although the mechanical properties of this α-phase have not been investigated.[63]

Understanding ω-assisted precipitation of the α phase is key for tuning processing conditions and/or alloy content to achieve desired mechanical properties. In the last 20 years, this topic has been an active area of research, and APT has expanded the field of knowledge considerably.

In high-misfit systems where the ω phase has a cuboidal morphology, ledges between the β and ω phases drive the ω-to-α transformation.[32] In low-misfit systems, the nucleation sites for the α phase have been the subject of debate for years. Historically, three locations of α precipitation have been considered:

1. The α phase precipitates at some distance from the ω/β boundary.[85]
2. The α phase precipitates in the core of the ω phase.[42]
3. The α phase precipitates at the ω/β boundary.[40]

Azimzadeh and Rack[85] proposed that Al diffuses away from the ω phase into the β matrix in a low-cost β-Ti alloy, providing an α phase nucleation point at some distance from the ω phase, where it then grows toward—and looks like it is precipitating "in association" with—the ω phase. Against this view, Prima et al.[42] have presented concurrent ω/α phase images that suggest the α phase forms in the core of the ω precipitate. The α phase might prefer nucleating in the core of the ω phase as a result of the low amounts of β stabilizers present in the ω phase compared to the heavily stabilized surrounding β phase, and the transformation would most likely be a purely displacive reaction.[24,42] TEM images of α particles with ω super cells at both boundaries—which could provide evidence that the α phase nucleates in the ω phase core—have been presented by Ahmed et al.[40] Ahmed et al.'s [40] TEM images could also provide evidence for the α phase nucleating at the ω/β boundary because the α particles were coherent with both the β and ω particles. HRTEM images by Furuhara et al.[115] also suggest that the α phase nucleates at the ω/β boundary, although the α phase growing toward the boundary cannot be ruled out. Li et al.[25] presented images similar to Furuhara et al.[115], but they determined that the α phase did not nucleate in the β phase and grow toward the boundary through composition analysis. If the α phase had nucleated in the β phase, the β stabilizer concentrations in the α phase would be expected to decrease with time, which does not match experimental observations.[25] Chemical driving force calculations by Shi et al.[116] indicate that the cuboidal ω/β interface is the most favorable nucleation site for α phase, and subsequent HRSTEM work showed the presence of the α phase at the cuboidal ω/β interface as predicted. Li et al.[27] and Zheng et al.[32] have also presented images of the α phase that nucleated at the ω/β boundary, and the 3-D APT results in the work of Zheng et al.[32] show the association of the ω and α phases.

Another much-disputed topic is the dominant nucleation driving force for ω-assisted α formation. Recent studies proposed that the elastic stress associated with the coherent ω/β interface, compositional variation between ω_{iso} and the surrounding β phase, and/or dislocations migrating to or forming at the ω/β boundary could provide additional driving force to promote the precipitation of the α phase.[21,22,116] A combination of those reasons could also influence α precipitation. To ascertain the key nucleation driving force for ω-assisted α formation, the transitional stage before and after α forms must be identified. Li et al.[27] captured the transitional stage by analyzing samples aged for 2, 4, 8, 12, 16, 24, 32, 48, and 192 h, respectively, at 573 K using HRTEM and APT. They found that high elastic stress and O-rich regions present around the coherent incommensurate-ω/β interface (at 12 h) do not assist α formation (see Figure 6).[27] The α phase forms only when the coherent interface becomes semi-coherent, suggesting that increased interfacial energy serves as the dominant factor in triggering ω-assisted α precipitation.[27] In addition, O trapped by ledges at the semi-coherent interfaces could provide an additional nucleation driving force for ω-assisted α formation. These results are supported by the chemical driving force calculations of Shi et al.[116] which indicate that a semi-coherent β/ω interface provides a lower energy barrier to α phase nucleation than a coherent interface. However, while Shi et al.[116] indicate that local enrichment of O at the ω/β interface could provide another chemical driving force for α nucleation, they also argue that the energy associated with other factors could outweigh the contribution of O and that more study is needed. Similarly to Shi et al.,[116] Nag et al.[110] concluded that coherency strains and local enrichment of Zr both played a role in the nucleation and growth of α precipitates at the ω/β interface. Zheng et al.[22] also conclude from CALPHAD studies that composition variance and coherency stress between the β and ω phases both play a role in α nucleation. Thus, there is a lack of current consensus and more experimental

evidence combined with modeling studies are required to determine the key nucleation driving force behind ω-assisted α formation.

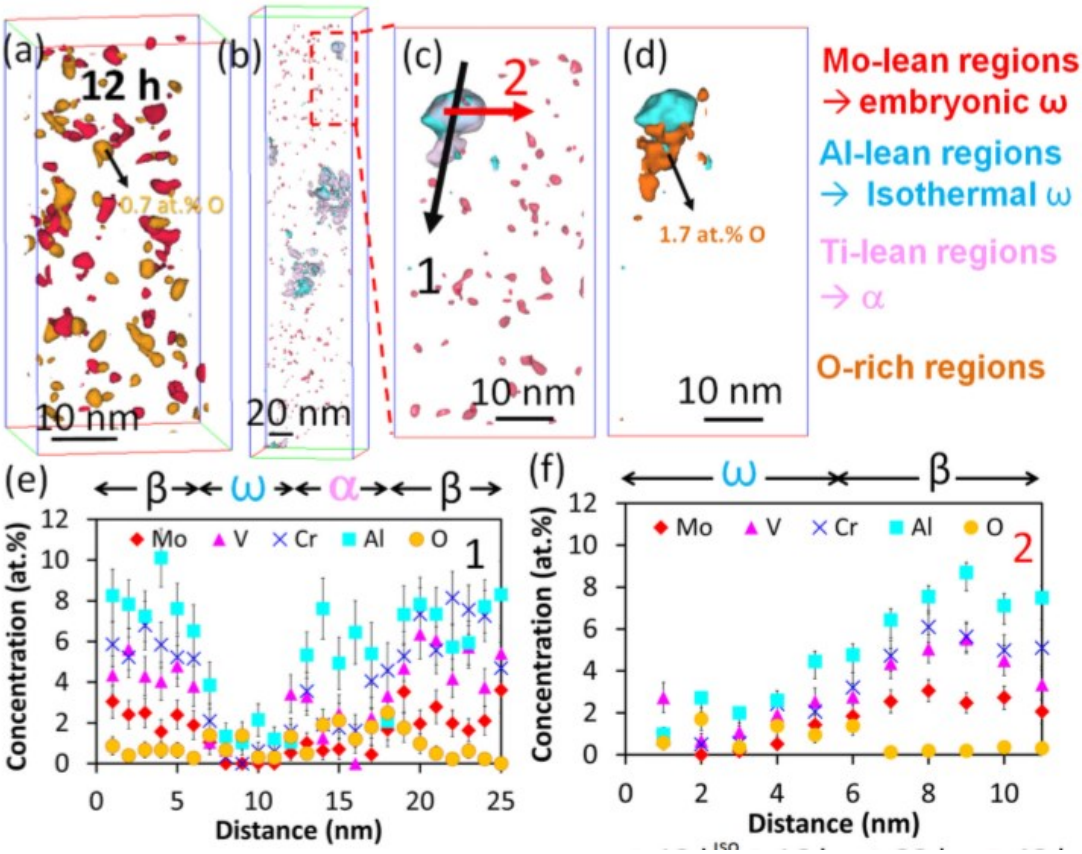

Figure 6. APT reconstructions of a Ti-6554 sample showing the relative positions of orange O-rich regions compared to (a) Mo-lean regions in red (embryonic ω phase) and (b) Al-lean regions in blue (isothermal ω phase) and Ti-lean regions in pink (α phase). A close-up region of (b) is shown in (c) and (d) highlighting the Al-lean and Ti-lean regions in (c) and the same Al-lean regions along with the O-rich regions in (d). The concentration profile in (e) was made using Arrow 1 in (c), and the profile in (f) was made using Arrow 2 in (c).

Furthermore, conclusions about O's role in α phase nucleation have led to debate on O's significance in ω-assisted α nucleation. While O increases the range of α phase stability in Ti alloys,[1] it also suppresses the formation of ω_{iso}. O suppresses ω_{iso} by pinning the linear defects that initiate the $(111)_\beta$ plane collapse[29] and/or by increasing the relative energy of the ω phase and the energy barrier for the β-to-ω transition.[117] Therefore, Li et al.'s[30] analysis that O-rich regions were near the ω phase, and that those O-rich regions could drive α-phase nucleation, was novel. Li et al.'s[30] claims are supported by Coakley et al.'s[118] results of a 27% higher concentration of O at the ω/β boundary compared to the β matrix. O-rich regions have also been found near Mo-lean embryonic ω particles,[80] and Coakley et al.[87] observed O-enrichment at the ω/β boundary starting after 1 hr of 300 °C heat treatment of Ti-5Al-5Mo-5V-3Cr. Within ω-phase particles, Niinomi et al.[94] have found a higher concentration of O than in the surrounding β matrix, although the association between O, the ω phase, and the α phase was not reported. Contradictory to those results, Zheng et al.[22,32,95] did not find a significant difference in O concentration

moving from the β phase to the ω phase. Instead, compositional differences of the other alloying elements and strains at the ω/β boundary are presented as the driving force—instead of O—by these studies.

6. Challenges in ω phase composition analysis

The differing results about O's role in α phase formation, along with the differing results about the composition of athermal and incommensurate ω_{iso} phase outlined above, could be because of the varying alloy compositions used by the different studies and lack of worldwide standardized approaches for APT data analysis procedures, especially when it comes to analyzing minor impurity element concentrations. Comparing the alloys used in 22 studies by Mo-Eq, 15 different Mo-Eq's were investigated as shown in Table 1. It is clear that comparisons of mechanisms are not usually made between alloys with similar Mo-Eq's. For example, Ahmed et al.[40] compared their ω_{ath} composition results from a Ti-5Al-5Mo-5V-2Cr-1Fe (Mo-Eq of 9.45) alloy to Devaraj et al.'s[20] results for a Ti-18Mo alloy (Mo-Eq of 18). Along with different Mo-Eq's, Ahmed et al.'s[40] alloy is more complex than the binary Ti-18Mo alloy. Stabilizer types are not consistent either, with some studies using alloys of four or more alloying elements of isomorphous- and eutectoid-type stabilizers, while others use binary isomorphous systems. Additionally, trace impurity elements are also found in the alloys which are not included in the Mo-Eq calculation. The presence of these elements, while small, could affect the phase transformations and are not always included in the APT data analysis.

Table 1. Molybdenum equivalencies of alloys used in APT studies.

Alloy	Mo equivalency	Trace elements present	Reference
Ti-6Al-4V	−3.32	Fe, C, N, O, H	[44]
Ti-18Mo	18	O	[20,43,72,93,95]
Ti-18Mo-5Al	13	O	[95]
Ti-10V-6Cu*	11.32	Not reported	[71]
Ti-5Al-5Mo-5V-3Cr	8.15	Fe, C, N, O, H	[22,82,87]
Ti-5Al-5Mo-5V-3Cr-0.5Fe	12.8	Not reported	[28]
Ti-5Al-5Mo-5V-2Cr-1Fe	9.45	O	[40,119]
Ti-6Cr-5Mo-5V-4Al	13.95	O	[25,27,30,80]
Ti-1Al-8V-5Fe	18.86	C, N, O	[5]
Ti-29Nb-13Ta-4.6Zr	10.98	O	[94]
Ti-38Nb-2Ta-3Zr	11.08	Not reported	[83]
Ti-24Nb-4Zr-8Sn	6.72	O	[120–123]
Ti-24Nb-3Mo-3Zr-2Sn	9.72	H	[124]
Ti-12Mo	12	O	[72]
Ti-20V	13.4	O	[32]
Ti-12V-2Fe-1Al	12.84	Not reported	[125]
Ti-34Nb-7Zr-7Ta	11.06	O	[110]

*Coefficient of 0.77 used for Cu calculated using the method described by Bania.[53]

Along with alloy composition, the APT experimental procedure can affect the reported compositions and spatial accuracy of APT results. Coakley et al.[118] have addressed this by comparing their results to those of Li et al.,[25] explaining how higher sample temperatures and laser energies make quantitative concentration analysis more difficult and increase the potential for surface diffusion, which affects spatial accuracy. Other studies, however, have not addressed how experimental procedures can affect results. This can be seen in Ahmed et al.'s[40] comparison to Devaraj et al.'s[20] work; Ahmed et al.[40]

did not mention that they used pulsed-laser-assisted APT and that Devaraj et al.'s[20] work used pulsed-voltage APT. In APT studies of the ω phase, the biggest differences in experimental procedure are the pulsing mode (pulsed laser vs. pulsed voltage), operating temperature, and laser pulse energies. The APT experimental parameters used for a selection of ω phase studies in β-Ti alloys are shown in Table 2. Unfortunately, not all settings are reported in the literature for pulsed-laser-assisted APT.

Table 2. Experimental procedure settings used for 19 different APT studies of the ω phase.

APT mode	**Operating temp.**	**Evaporation rate**	**Voltage pulse fraction**	**Laser wavelength**	**Pulse rate**	**Pulse energy**	**Laser spot size**	**Ref.**
Voltage	60 K	0.2–1.0%	20%					[22,32]
Voltage	60 K	0.5–0.7%	20%					[95]
Voltage	70 K	0.2–1.0%	20%					[20,43,71,93,110]
Voltage	70 K	0.2–1.0%	30%					[28]
Voltage	80 K	0.5–0.8%	10%					[94]
Laser	60 K		0.005 ions/pulse	355 nm		20 pJ		[5]
Laser	50 K		0.005 ions/pulse	355 nm	250 kHz	70 pJ	2 µm	[40]
Laser	50 K		0.005 ions/pulse		250 kHz	70 pJ	2 µm	[25]
Laser	50 K		0.005 ions/pulse			80 pJ		[27]
Laser	50 K					80 pJ		[30,80]
Laser	40 K			355 nm		50 pJ		[82]
Laser	40 K			512 nm		200 pJ		[82]
Laser					250 kHz	50 pJ		[125]

Both voltage pulsing and laser pulsing of APT has been used to analyze β-Ti alloys. In both voltage and laser modes, higher specimen temperatures or higher laser energies can provide better yield but poorer spatial resolution as a result of surface migration. Coakley et al.[87] found that higher laser pulse energies reduced the volume fraction of the ω phase that is identified in a sample, as shown in Figure 7. Coakley et al.[87] have also found that laser direction can influence detection of the ω phase in Ti samples, with ω-phase particles on the same side as the laser being more difficult to detect.

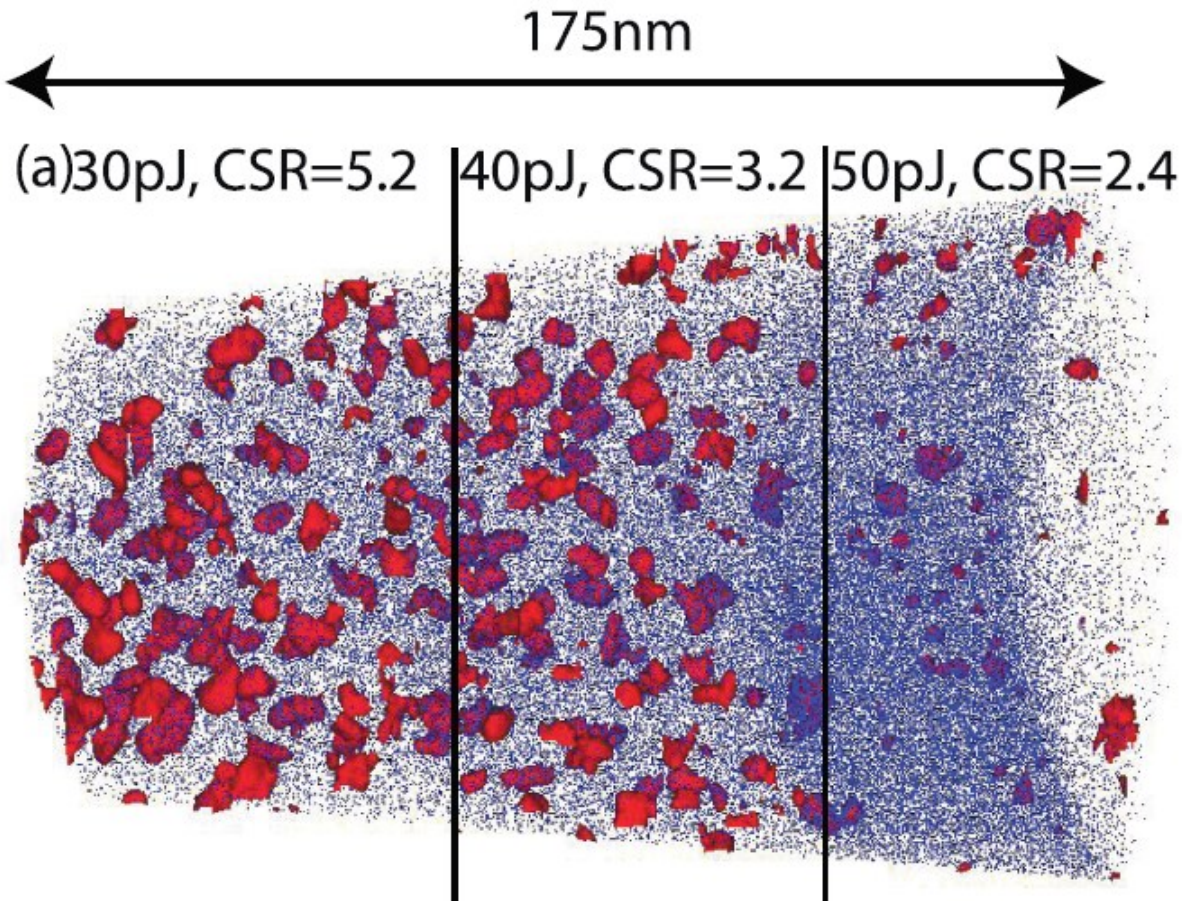

Figure 7. An APT sample reconstruction showing how higher laser energy reduces the volume fraction of the ω phase detected in β-Ti alloys through a stepped increase in laser energy during a single APT experiment. The red volumes indicate the Ti-rich ω phase. Adopted from J. Coakley, A. Radecka, D. Dye, P. A. Bagot, T. L. Martin, T. J. Prosa, Y. Chen, H. J. Stone, D. N. Seidman and D. Isheim, "Characterizing nanoscale precipitation in a titanium alloy by laser-assisted atom probe tomography," *Materials Characterization,* vol. 141, pp. 129–138, 2018.

Finally, when it comes to using APT to analyze the composition of ω, β, and α phases, the procedure selected for ranging the mass-to-charge spectra peaks of minor impurity elements such as O can induce a significant amount of statistical variability. For example, the O^{+1} peak at 16 Da can overlap with the Ti^{3+} peak, requiring a detailed peak deconvolution. TiO molecular peaks are often minor and may not be indexed if the mass-to-charge spectra ranging is not conducted using a log scale for the counts. Such variability in data analysis procedures must be accounted for to facilitate accurate interpretation of the roles of minor impurity elements such as O in key phase transformation mechanisms in alloys.

Thus, the different alloy compositions, variabilities in APT experimental parameters used, and APT mass-to-charge spectra ranging procedures used in the research for ω phase transformation in β titanium alloys can make it difficult to conclusively use only the current body of work to resolve the debates around the ω-phase transformation.

7. Effect of the ω phase on mechanical properties

A single crystal ω phase is difficult to grow without high pressures, so the mechanical properties of a single crystalline ω phase have been determined using simulations and polycrystalline material. Tane et al.[62] used HPT to create a polycrystalline ω microstructure to determine the mechanical properties of the ω phase because the elastic tensor was calculated using simulations but had never been verified experimentally. The ω phase was anisotropic, with the <0001> direction modulus equal to 201 ± 7.4 GPa and the <11-20> direction modulus being 70 GPa lower at 129 ± 3.9GPa.[62] The experimental ω-phase elastic tensor agreed well with the simulated elastic tensor calculated using the tight-binding model[126] (shown in Table 3), and an experimental isotropic elastic modulus was calculated to compare to the β phase.[62] While direct comparison to pure Ti with the bcc structure at RT is not possible, the β values at 1293K are included. Also included are a range of property values compiled from multiple β alloys (β III, β C, Ti-1023, Ti-13V-11Cr-3Al, Ti-15V-3Cr-3Al-3Sn, Ti-8Mo-8V-2Fe-3Al, Ti-15Mo-5Zr, Ti-15Mo-5Zr-3Al, Ti-8V-5Fe-1Al, and Ti-16V-2.5Al) at RT, both as-quenched and aged, since processing can significantly affect the mechanical properties of β alloys. More detail on aging treatments and corresponding modulus values for specific alloys can be found in the Materials Properties Handbook: Titanium Alloys[8].

Table 3. The elastic and shear modulus of the ω and β phases.

Phase	Temperature (K)	E_{iso} (GPa)	G_{iso} (GPa)	Reference
ω (simulation)	0	155	61	[62]
ω (polycrystalline)	RT	152.8 ± 0.6	60.1 ± 0.3	[62]
β	1293K	65	23	[127]
β (as-quenched)	RT	78-103	34-43	[8]
β (Aged)	RT	100-124	40.7-43.3	[8]

While it is difficult to compare these moduli because of the variability in temperatures, the experimental ω phase elastic modulus is approximately 30 GPa higher than the highest modulus reached for β-Ti alloys, and the shear modulus is approximately 17 GPa higher than the highest β-Ti shear modulus. Therefore, the elastic and shear modulus of the ω phase should contribute to an increase in the elastic modulus of β-Ti alloys when the ω phase is present. Hsu et al.[128] and Ho et al.[129] have observed this, recording increases in the bending elastic modulus of ~35 GPa and ~20–40 GPa, respectively. Coakley et al.[87] and Hsu et al.[97] also report an elastic modulus increase as indicated by the increase in slope in the elastic region of their tensile and bending tests, given in Figure 8.[129] However, this apparent increase is not observed for athermal ω microstructures. ω_{ath} tends to be neglected in studies on the mechanical influence of the ω phase because it is generally thought not to affect the mechanical properties of β-Ti alloys.[8,21,69] Unfortunately, because ω_{ath} cannot be prevented during quenching of metastable or near-β alloys without changing the alloy composition to stabilize the β phase,[28,130] the mechanical properties of β alloys with and without ω_{ath} (such as Ti-15Mo with ω_{ath} and Ti-15Mo without ω_{ath}) cannot be compared.[21] It is possible that ω_{ath} does affect mechanical properties—one study by Ho[130] reports an increase in microhardness from 263 Hv to 337 Hv associated with the presence of ω_{ath}. No extensive studies on the mechanical effects of the incommensurate ω phase have been done so far.

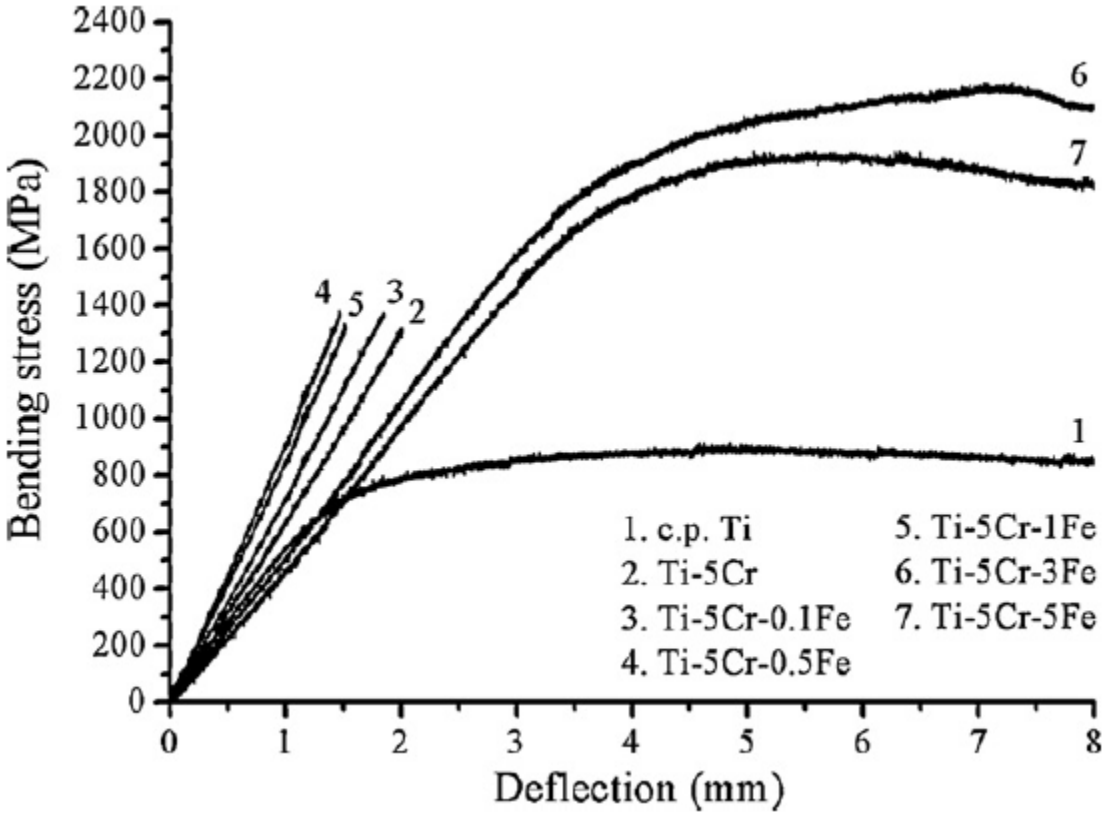

Figure 8. Bending test results showing the elastic modulus increase in β-Ti with ω-phase microstructures. Adopted from Ho, W.-F., Pan, C.-H., Wu, S.-C., et al. "Mechanical properties and deformation behavior of Ti–5Cr–xFe alloys," Journal of Alloys and Compounds, V. 472, Nos. 1–2, 2009, pp. 546–50.

Along with an increase in the elastic modulus, the ω phase increases the microhardness of β-Ti alloys. Multiple studies have reported an increase in microhardness after precipitation of the isothermal ω phase, regardless of alloy composition.[74,76,87,89,97,104,128,131–134] Although Jones et al.[69] attribute the microhardness increase to precipitation of the nanoscale α phase, Coakley et al.[74] counter that the observed hardness increase from 280 Hv to 400 Hv was due to the rapid precipitation of ω_{iso} during a 400 °C heat treatment. ω phase microstructures have also exhibited higher microhardness than martensitic α'' microstructures by approximately 100 Hv,[97] although the hardness of α'' martensite is not wholly intrinsic and is partly due to sliding interfaces. Hida et al.[76] found that hardness increased with precipitation of the commensurate ω phase, as shown in Figure 9. The results in Figure 9 also support the assumption stated above that the incommensurate ω phase does not affect the mechanical properties of β alloys because the incommensurate ω phase did not appear to affect microhardness.[76] Figure 9 is also a typical example of the scale of hardness increase, as most hardness values were reported to start around 300 Hv and increase to 400–550 Hv.[74,76,89,97,128,132–134]

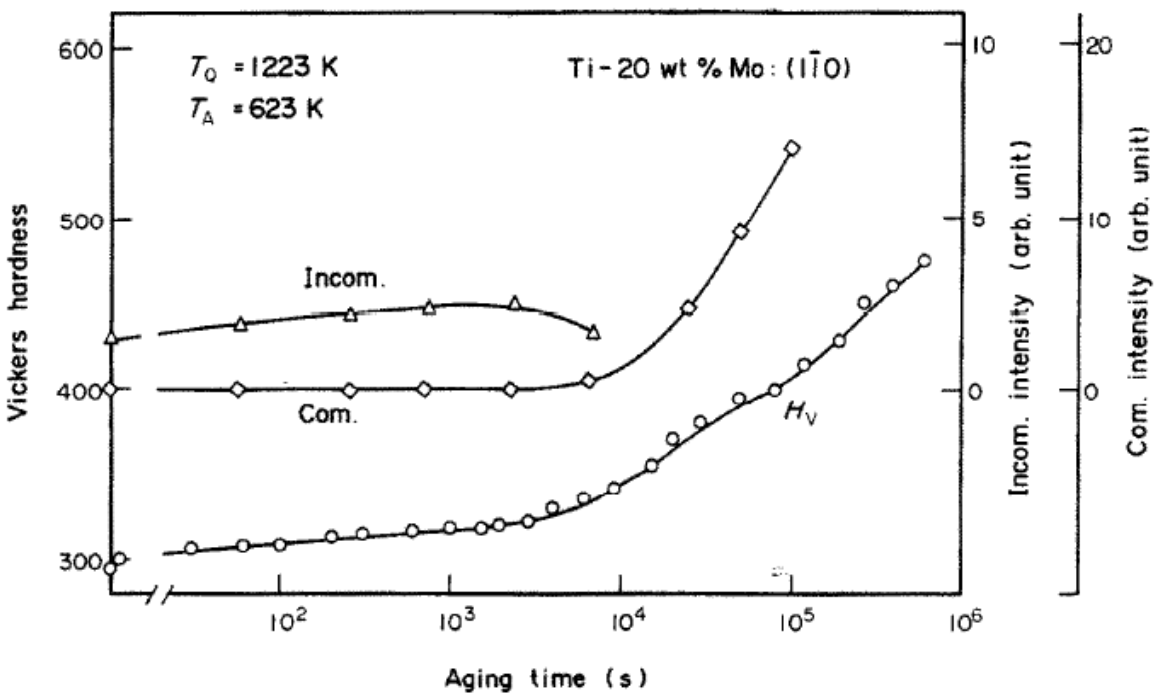

Figure 9. The effects of incommensurate and commensurate ω phases on the microhardness of a Ti-20Mo alloy. Adapted from M. Hida, E. Sukedai and H. Terauchi, "Microscopic approaches to isothermal transformation of incommensurate ω phase zones in Ti-20wt%Mo alloy studied by XDS, HREM and EXAFS," *Acta Metallurgica,* vol. 36, no. 6, pp. 1429–1441, 1988.

The ω-phase microstructure also increases the tensile strength of alloys. Chandrasekaran et al.[135] found that precipitating ω_{iso} in a Ti-15Cr (at%) alloy increased the yield strength of the alloy by ~186 MPa, and Mantri et al.[112] found that ω_{iso} precipitation increased the UTS of Ti-12Mo by ~525 MPa. Feeney and Blackburn[136] found that β + ω microstructures in a Ti-11.5Mo-6Zr-4.5Sn alloy exhibited strengths up to 1500 MPa. Williams et al.[137] found that the yield strength of Ti-10Mo (at%), Ti-25V (at%), Ti-8Mn (at%), and β III alloys increased when the ω phase was present and decreased when the α phase became the dominant phase. Alloys that deform via the ω transformation also exhibit higher yield strengths than alloys that deform via twins.[51]

The increase in elastic modulus and tensile strength due to the ω phase is accompanied by embrittlement. In tension, embrittlement is shown by a decrease in elongation to failure (ε_f) when ω microstructures are present, as Zhao et al.,[31] Mantri et al.,[112] Williams et al.,[137] Wang et al.,[125] and Feeney and Blackburn[136] documented in alloys that had precipitated the isothermal ω phase. The decrease can be seen the most clearly in Zhao et al.'s[31] Ti-18V alloy in Table 4 and is also demonstrated by the drop in ε_f from ~35% to < 5% with ω_{iso} precipitation in Mantri et al.'s[112] Ti-12Mo alloy. Li et al.[88] has shown that ε_f in tensile deformation is dependent on the presence of the isothermal ω phase, with higher ω_{iso} volume fractions corresponding to lower elongation to failure values. A drop in ε_f from 6.1% to ~1.7% in a Ti-24Nb-4Zr-8Sn alloy was associated with the presence of isothermal ω phase microstructures.[131] Chandrasekaran et al.[41] also observed a drop in ε_f from 17% to 2% when ω_{iso} was precipitated. When the ω phase was removed from the β matrix using heat treatments, the ε_f increased from 2% to 6%.[135] These embrittling effects are only true for ω_{iso} microstructures because ω_{ath} does not embrittle alloys like ω_{iso}; Wang et al.[138]

and Sun et al.[106] observed no embrittling effects in binary Ti-Mo alloys. Chandrasekaran et al.[135] have also found that ω_{ath} microstructures reach an ε_f of 13%, while ω_{iso} microstructures reached 2%.

Table 4. The strengths and ε_f of β and β + ω phase microstructures.[31]

Alloy	Microstructure	approx. 2% Yield Stress (MPa)	approx. UTS (MPa)	approx. ε_f (%)
Ti-18V	β+ω_{ath}	730	830	28
Ti-18V	β+ω_{ath}+deformation ω	750	1080	6
Ti-20V	β+ ω_{ath}	880	910	17
Ti-20V	β+ω_{ath}+deformation ω	900	1050	10
Ti-22V	β	910	900	11
Ti-22V	β+deformation ω	950	980	10

Bending tests also illuminate the embrittling effects of the ω phase. Hsu et al.[97] and Ho et al.[129] found that alloys with ω-phase microstructures fractured during bending at significantly lower deflections than alloys containing the ω + α or no ω phase microstructures. This can be seen in the low deflections at the fracture of ω-phase microstructures (Alloys 2–5) in Figure 8, compared to Alloys 1, 6, and 7, which completed the bending test without fracture.[129] Cleavage facets were found on the fracture surfaces of the ω-phase microstructures,[97,129] which are characteristic of decreased ε_f.

The embrittling effects of the ω phase are thought to be because dislocations stop or bend around ω particles, leaving high dislocation densities in the β matrix.[137] When dislocations do move through the ω phase, they shear the ω phase, creating slip bands that can lead to crack nucleation at low macroscopic strains,[139] as shown in Figure 10. Recently, Lai et al.[83] have shown that high densities of nanometer-sized (~1.23 nm) ω phases suppress TWIP and TRIP effects, and Wang et al.[125] have shown that ω_{iso} changes the deformation mode from deformation twinning to slip+deformation twinning to slip+stress-induced ω phase transformation to brittle fracture as it grows in size. TWIP and TRIP deformations have been shown to lead to a desirable balance of strength and ε_f in β alloys,[140] and the ω phase suppression of these effects leads to localized plasticity in dislocation channels and reduction of ε_f values.[83] Sun et al.[106] have used low heat-treatment temperatures and 60 second heat treatment times to avoid embrittlement while strengthening their Ti-12Mo alloy through precipitation of ω_{iso}. Their study pointed to diffusion being another cause of embrittlement because the processing route was meant to precipitate ω_{iso} without allowing significant diffusion between the ω and β phases.[106] When diffusion did not occur, strengthening of the alloy from ω_{iso} was achieved but the true strain at the fracture was still over 40%. When diffusion occurred, the tensile strength of the alloys was observed to be highest, but the embrittling effects were also seen manifested by the reduction of true strain at fracture to ~3%.[106]

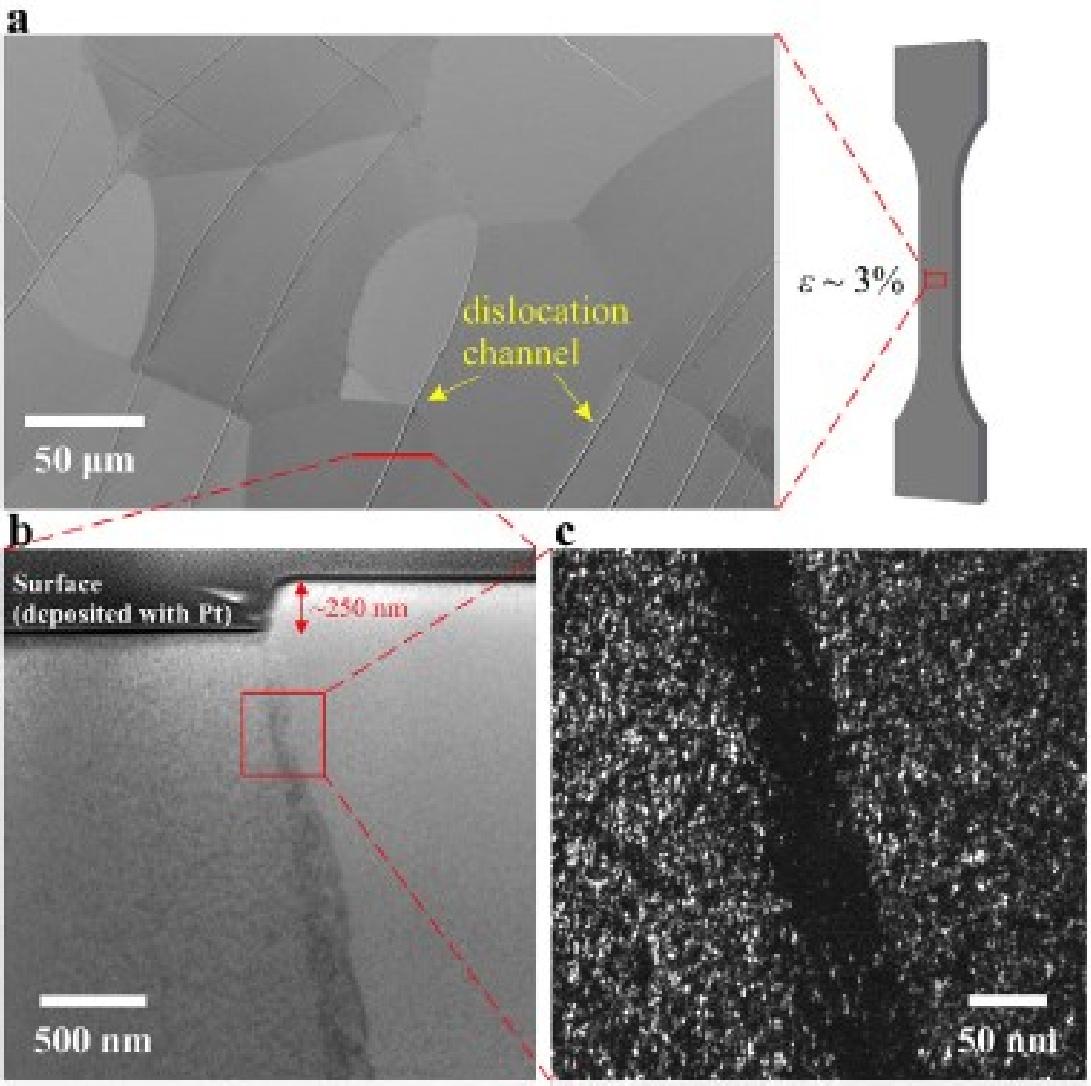

Figure 10. TEM micrographs of deformed β alloys showing dislocation channels that are ω-phase free. Adapted from M.J. Lai, T. Li, and D. Raabe, "ω phase acts as a switch between dislocation channeling and joint twinning- and transformation-induced plasticity in a metastable beta titanium alloy," *Acta Materialia*, vol. 151, pp. 67–77, 2018.

Because the ω phase allows crack nucleation at low macroscopic strains, it can be detrimental to fatigue properties.[139] However, ω_{iso} microstructures have been found to retard fatigue crack propagation significantly more than α-phase microstructures.[141] Nakai et al.[133] have also found that the maximum cycle stress of their TNTZ alloy increased by ~200 MPa after precipitation of the ω phase through a combination of cold-rolling and aging. In Feeney and Blackburn's[136] study, the fracture toughness of the β-Ti alloy was independent of ω particle size once the particles were larger than ~ 10 nm.

Although crack nucleation and embrittlement are why processing routes and alloy compositions are designed to avoid precipitation of the ω phase, ω-assisted α-phase microstructures have attractive mechanical properties. The ω phase can also influence the mechanical properties of β alloys by preventing the formation of the martensitic α'' phase,[16,23] which is detrimental to the formability of β alloys.[142]

The tensile behavior of β alloys is heavily affected by the size, morphology, and distribution of α-phase particles in the β matrix, and fine-grained α-phase microstructures have exhibited high strengths with higher ε_f than ω-phase microstructures.[143] Azimzadeh and Rack[85] found that the hardness of a Ti-6.8Mo-4.5Fe-1.5Al alloy (TIMET LCB alloy) was highest with a combination ω phase and α phase microstructures. Hsu et al.[97] and Ho et al.[129] found that alloys with ω + α phase microstructures could withstand more deflection before fracture in bending tests than alloys with only ω phase microstructures. ω-assisted α-phase microstructures have been found to be weaker than ω_{iso} microstructures, as Williams et al.[137] showed when the yield strength of Ti-10Mo (at%) dropped by ~275 MPa with precipitation of the α phase; however, the strength was still relatively high at ~965 MPa, and the ε_f increased from 6% to 8%. The mechanical property benefits of the ω-assisted α phase are driving research of processing routes that encourage ω_{iso} to form the ω-assisted α phase.[22,27,32,40,42,113]

8. Conclusions and future directions for research

With β-Ti's useful attributes of a high strength-to-weight ratio, good corrosion resistance, and a low elastic modulus, it is important to understand the phase transformations that affect its mechanical properties. An important transformation is the β-to-ω transformation, both because of its direct effects on the mechanical properties of β-Ti alloys and its influence on other phase transformations.

Quenching can precipitate both commensurate and incommensurate ω phases. Low-temperature heat treatments precipitate the isothermal ω phase as well-distributed ellipsoidal or cuboidal particles. Temperature and time can be used to influence the amount, size, volume fraction, and composition of ω_{iso}. ω_{iso} is known to assist in the formation of a fine-grained α-phase microstructure. Cuboidal ω_{iso} particles have ledges that act as nucleation points for the α phase. The deformation-induced ω phase can increase the strength of β alloys and has the potential to be used in HPT processing.

β-Ti alloys with ω-phase microstructures exhibit higher strengths, microhardness, and elastic moduli than β-Ti alloys without the ω phase. The elongation to failure of β alloys also decreases when ω-phase microstructures are present, which limits the application of ω-phase microstructures. Recent work has suggested that the composition of the ω phase is linked to the embrittling effects and that there is potential to reach high strengths using the ω phase without significantly compromising ε_f; however, determining the underlying reason for the embrittling effect of the isothermal ω phase is still a future challenge.

Other unresolved questions in the ω-phase field are the exact role that oxygen plays in α-phase nucleation, how ellipsoidal ω_{iso} particles assist α-phase nucleation, and whether commensurate and incommensurate athermal ω phases preferentially nucleate at stabilizer-lean pockets in β alloys. These questions are currently driving research in this field.

To investigate these questions, studies of binary alloy systems, such as Ti-Cr, could be used to see how alloy chemistry affects formation of the ω phase and subsequent formation of the α phase. Research into how eutectoid stabilizers affect the composition of the ω phase is another avenue that merits investigation, especially because APT composition studies have mostly focused on isomorphous systems. Work on eutectoid stabilizers could also help with understanding ω-phase formation in complex alloy systems that contain both isomorphous and eutectoid stabilizers. Also, taking a relatively well-understood system such as Ti-Mo and systematically increasing its complexity with the addition of other alloying elements (such as Fe and Al) would also be valuable for understanding how each element individually affects ω phase formation. Modeling has also been a powerful tool to understand the driving forces of the β-to-ωphase transformation, and could be applied to determine the effects of individual alloying elements

on this transformation. Using modeling together with experimental results could help achieve a fundamental understanding of the different effects of alloying elements on ω phase formation, in particular the differences in isomorphous and eutectoid β-stabilizers.

Studies to find evidence of O-enrichment at the ω/β boundary in more alloy systems would also be useful. In conjunction with this, studying how alloy composition and APT experimental settings and data analysis procedures affect O concentration and location in β-Ti alloys could also help clarify the reasons for O-enrichment reported at the ω/β boundary in some studies and not in others. Consistent standards for APT analysis could allow for a more systematic approach to investigating the influence of O on the ω-assisted α phase transformation in the future. Adopting consistent standards would also help in comparing the results of different studies, as currently it is difficult to systematically compare APT results from different research groups without addressing the differences in analysis as discussed in this work.

In general, more work on how the ω phase influences fatigue behavior of β-Ti alloys is needed. Specifically, crack initiation and propagation studies would be meaningful contributions to the body of work on the ω phase.

Moving forward in ω-phase research, work to resolve these debates will continue helping researchers tune processing pathways and alloy compositions to achieve desired microstructures and mechanical properties in β-Ti.

Acknowledgements

This work was made possible through the support of the U.S. Department of Energy, Office of Science, Office of Workforce Development for Teachers and Scientists, Office of Science Graduate Student Research (SCGSR) program. The SCGSR program is administered by the Oak Ridge Institute for Science and Education for the DOE under contract number DE-SC0014664. A portion of the funding for this research was supported by the National Science Foundation Division of Material Research, under Grant No. DMR-1607942 through the Metals and Metallic Nanostructures (MMN) program (JB & CJB). A portion of the funding for this research was supported by the US Department of Energy, Office of Basic Energy Science through grant No. DE-SC0001525 (JB & CJB). AD would like to acknowledge the funding from the Laboratory Directed Research and Development program as a part of the Solid Phase Processing Initiative at Pacific Northwest National Laboratory (PNNL).

References

1. Lütjering, G., and Williams, J. C. “Titanium,” 2nd edition, Berlin, Springer, 2007, 442 pp.
2. Immarigeon, J. P., Holt, R. T., Koul, A. K., et al. “Lightweight materials for aircraft applications,” *Materials Characterization*, V. 35, No. 1, 1995, pp. 41–67.
3. Cotton, J. D., Briggs, R. D., Boyer, R. R., et al. “State of the Art in Beta Titanium Alloys for Airframe Applications,” *JOM*, V. 67, No. 6, 2015, pp. 1281–303.
4. Kolli, R., and Devaraj, A. “A Review of Metastable Beta Titanium Alloys,” *Metals*, V. 8, No. 7, 2018, p. 506.
5. Devaraj, A., Joshi, V. V., Srivastava, A., et al. “A low-cost hierarchical nanostructured beta-titanium alloy with high strength,” *Nature Communications*, V. 7, No. 1, 2016, p. 11176.
6. Niinomi, M., and Boehlert, C. J. “Titanium Alloys for Biomedical Applications.” In: Niinomi, M., Narushima, T., Nakai, M., eds. Advances in Metallic Biomaterials: Tissues, Materials and Biological Reactions. Berlin, Heidelberg, Springer Berlin Heidelberg, 2015. pp. 179–213.
7. “The Nation’s Older Population Is Still Growing, Census Bureau Reports,” *Press Release CB17-100*, 2017.

8. Boyer, R., Welsch, G., and Collings, E. W. “Materials properties handbook: titanium alloys,” 4th edition, Materials Park, Ohio, ASM International, 2007, 1176 pp.
9. Frost, P. D., Parris, W. M., Hirsch, L. L., et al. “Isothermal transformation of titanium-chromium alloys,” *Trans. Amer. Soc. metals*, V. 46, 1954, pp. 231–56.
10. Jamieson, J. C. “Crystal Structures of Titanium, Zirconium, and Hafnium at High Pressures,” *Science*, V. 140, No. 3562, 1963, pp. 72–3.
11. Vohra, Y. K., and Spencer, P. T. “Novel γ -Phase of Titanium Metal at Megabar Pressures,” *Physical Review Letters*, V. 86, No. 14, 2001, pp. 3068–71.
12. Hsiung, L. M., and Lassila, D. H. “Shock-induced deformation twinning and omega transformation in tantalum and tantalum–tungsten alloys,” *Acta Materialia*, V. 48, No. 20, 2000, pp. 4851–65.
13. Hickman, B. S. “The formation of omega phase in titanium and zirconium alloys: A review,” *Journal of Materials Science*, V. 4, No. 6, 1969, pp. 554–63.
14. Sikka, S. K., Vohra, Y. K., and Chidambaram, R. “Omega phase in materials,” *Progress in Materials Science*, V. 27, Nos. 3–4, 1982, pp. 245–310.
15. Ikeda, Y., and Tanaka, I. “Stability of the ω structure of transition elements,” *Physical Review B*, V. 93, No. 9, 2016, p. 094108.
16. Silcock, J. M., Davies, M. H., and Hardy, H. K. “Structure of the ω-Precipitate in Titanium–16 per cent Vanadium Alloy,” *Nature*, V. 175, No. 4460, 1955, p. 731.
17. Kolli, R. P., Joost, W. J., and Ankem, S. “Phase Stability and Stress-Induced Transformations in Beta Titanium Alloys,” *JOM*, V. 67, No. 6, 2015, pp. 1273–80.
18. Williams, J. C., de Fontaine, D., and Paton, N. E. “The ω-Phase as an Example of an Unusual Shear Transformation,” *Metallurgical Transactions*, V. 4, 1973, pp. 2701–8.
19. de Fontaine, D., and Buck, O. “A Monte Carlo Simulation of the Omega Phase Transformation,” *Philosophical Magazine*, V. 27, No. 4, 1972, pp. 967–83.
20. Devaraj, A., Nag, S., Srinivasan, R., et al. “Experimental evidence of concurrent compositional and structural instabilities leading to ω precipitation in titanium–molybdenum alloys,” *Acta Materialia*, V. 60, No. 2, 2012, pp. 596–609.
21. Duerig, T. W., Terlinde, G. T., and Williams, J. C. “Phase transformations and tensile properties of Ti-10V-2Fe-3Al,” *Metallurgical Transactions A*, V. 11, No. 12, 1980, pp. 1987–98.
22. Zheng, Y., Williams, R. E. A., Wang, D., et al. “Role of ω phase in the formation of extremely refined intragranular α precipitates in metastable β-titanium alloys,” *Acta Materialia*, V. 103, 2016, pp. 850–8.
23. Ohmori, Y., Ogo, T., Nakai, K., et al. “Effects of ω-phase precipitation on β→α, α'' transformations in a metastable β titanium alloy,” *Materials Science and Engineering A*, 2001, p. 7.
24. Prima, F., Vermaut, P., Ansel, D., et al. “ω Precipitation in a Beta Metastable Titanium Alloy, Resistometric Study,” *Materials Transactions, JIM*, V. 41, No. 8, 2000, pp. 1092–7.
25. Li, T., Kent, D., Sha, G., et al. “New insights into the phase transformations to isothermal ω and ω-assisted α in near β-Ti alloys,” *Acta Materialia*, V. 106, 2016, pp. 353–66.
26. Wang, Y. B., Zhao, Y. H., Lian, Q., et al. “Grain size and reversible beta-to-omega phase transformation in a Ti alloy,” *Scripta Materialia*, V. 63, No. 6, 2010, pp. 613–6.
27. Li, T., Kent, D., Sha, G., et al. “Nucleation driving force for ω-assisted formation of α and associated ω morphology in β-Ti alloys,” *Scripta Materialia*, V. 155, 2018, pp. 149–54.
28. Nag, S., Banerjee, R., Srinivasan, R., et al. “ω-Assisted nucleation and growth of α precipitates in the Ti–5Al–5Mo–5V–3Cr–0.5Fe β titanium alloy,” *Acta Materialia*, V. 57, No. 7, 2009, pp. 2136–47.
29. Qazi, J. I., Marquardt, B., Allard, L. F., et al. “Phase transformations in Ti–35Nb–7Zr–5Ta–(0.06–0.68)O alloys,” *Materials Science and Engineering: C*, V. 25, No. 3, 2005, pp. 389–97.
30. Li, T., Kent, D., Sha, G., et al. “The mechanism of ω-assisted α phase formation in near β-Ti alloys,” *Scripta Materialia*, V. 104, 2015, pp. 75–8.

31. Zhao, X., Niinomi, M., Nakai, M., et al. “Effect of Deformation-Induced ω Phase on the Mechanical Properties of Metastable β-Type Ti-V Alloys,” *Materials Transactions*, V. 53, No. 8, 2012, pp. 1379–84.
32. Zheng, Y., Choudhuri, D., Alam, T., et al. “The role of cuboidal ω precipitates on α precipitation in a Ti-20V alloy,” *Scripta Materialia*, V. 123, 2016, pp. 81–5.
33. Yamamoto, A., and Tsubakino, H. “Convergent Beam Dark Field Imaging Technique with its Application to Observation of Multiphase Materials,” *Materials Transactions, JIM*, V. 39, No. 9, 1998, pp. 989–94.
34. Hatt, B. A., and Roberts, J. A. “The w-phase in zirconium base alloys,” *Acta Metallurgica*, V. 8, 1960, p. 10.
35. Samiee, A., Casillas, G., Ahmed, M., et al. “Formation of Deformation-Induced Products in a Metastable-β Titanium Alloy during High Temperature Compression,” *Metals*, V. 8, No. 2, 2018, p. 100.
36. Blackburn, M. J., and Williams, J. C. “Phase Transformations in Ti-Mo and Ti-V Alloys,” *Transactions of the Metallurgical Society of AIME*, V. 242, 1968, pp. 2461–9.
37. Ohmori, Y., Natsui, H., and Nakai, K. “Crystallographic Analysis of α Phase Formation in a Metastable β Ti Alloy,” *Materials Transactions, JIM*, V. 39, No. 1, 1998, pp. 49–56.
38. Aurelio, G., and Fernández Guillermet, A. “Interatomic distances of the hexagonal omega structure in Ti-V alloys: neutron diffraction study and analysis of bonding related regularities,” *Scripta Materialia*, V. 43, No. 7, 2000, pp. 665–9.
39. Bönisch, M., Panigrahi, A., Stoica, M., et al. “Giant thermal expansion and α-precipitation pathways in Ti-alloys,” *Nature Communications*, V. 8, No. 1, 2017, p. 1429.
40. Ahmed, M., Li, T., Casillas, G., et al. “The evolution of microstructure and mechanical properties of Ti–5Al–5Mo–5V–2Cr–1Fe during ageing,” *Journal of Alloys and Compounds*, V. 629, 2015, pp. 260–73.
41. Chandrasekaran, V., Taggart, R., and Polonis, D. H. “An electron microscopy study of the aged omega phase in Ti-Cr alloys,” *Metallography*, V. 11, No. 2, 1978, pp. 183–98.
42. Prima, F., Vermaut, P., Texier, G., et al. “Evidence of α-nanophase heterogeneous nucleation from ω particles in a β-metastable Ti-based alloy by high-resolution electron microscopy,” *Scripta Materialia*, V. 54, No. 4, 2006, pp. 645–8.
43. Nag, S., Devaraj, A., Srinivasan, R., et al. “Novel Mixed-Mode Phase Transition Involving a Composition-Dependent Displacive Component,” *Physical Review Letters*, V. 106, No. 24, 2011, p. 245701.
44. Fan, Z., and Miodownik, A. P. “TEM study of metastable β-phase decomposition in rapidly solidified Ti-6Al-4V alloy,” *Journal of Materials Science*, V. 29, 1994, pp. 6403–12.
45. Vohra, Y. K., Sikka, S. K., Vaidya, S. N., et al. “Impurity effects and reaction kinetics of the pressure-induced α → ω transformation in Ti,” *Journal of Physics and Chemistry of Solids*, V. 38, No. 11, 1977, pp. 1293–6.
46. Singh, A. K., Mohan, M., and Divakar, C. “The kinetics of pressure-induced α→ω transformation in Ti,” *Journal of Applied Physics*, V. 53, No. 2, 1982, pp. 1221–3.
47. Errandonea, D., Meng, Y., Somayazulu, M., et al. “Pressure-induced α→ω transition in titanium metal: a systematic study of the effects of uniaxial stress,” *Physica B*, V. 355, 2005, pp. 116–25.
48. Arul Kumar, M., Hilairet, N., McCabe, R. J., et al. “Role of twinning on the omega-phase transformation and stability in zirconium,” *Acta Materialia*, V. 185, 2020, pp. 211–7.
49. Liang, Q., Kloenne, Z., Zheng, Y., et al. “The role of nano-scaled structural non-uniformities on deformation twinning and stress-induced transformation in a cold rolled multifunctional β-titanium alloy,” *Scripta Materialia*, V. 177, 2020, pp. 181–5.

50. Ahmed, M., Wexler, D., Casillas, G., et al. “The influence of β phase stability on deformation mode and compressive mechanical properties of Ti–10V–3Fe–3Al alloy,” *Acta Materialia*, V. 84, 2015, pp. 124–35.
51. Wang, X. L., Li, L., Mei, W., et al. “Dependence of stress-induced omega transition and mechanical twinning on phase stability in metastable β Ti–V alloys,” *Materials Characterization*, V. 107, 2015, pp. 149–55.
52. Xing, H., and Sun, J. “Mechanical twinning and omega transition by ⟨111⟩ {112} shear in a metastable β titanium alloy,” *Applied Physics Letters*, V. 93, No. 3, 2008, p. 031908.
53. Bania, P. J. “Beta titanium alloys and their role in the titanium industry,” *JOM*, V. 46, No. 7, 1994, pp. 16–9.
54. Jaworski, A., and Ankem, S. “The Effect of α Phase on the Deformation Mechanisms of β Titanium Alloys,” *Journal of Materials Engineering and Performance*, V. 14, No. 6, 2005, pp. 755–60.
55. Hanada, S., and Izumi, O. “Correlation of Tensile Properties, Deformation Modes, and Phase Stability in Commercial/3-Phase Titanium Alloys,” *Metallurgical Transactions A*, 1986, p. 7.
56. Guibert, J. P., and Servant, C. “Deformation Mechanisms in a βm Alloy.” vol. 8. Birmingham, 1995.
57. Korneva, A., Straumal, B., Kilmametov, A., et al. “Omega Phase Formation in Ti–3wt.%Nb Alloy Induced by High-Pressure Torsion,” *Materials*, V. 14, No. 9, 2021, p. 2262.
58. Ivanisenko, Y., Kilamametov, A., Rösner, H., et al. “Evidence of α → ω phase transition in titanium after high pressure torsion,” *International Journal of Materials Research*, V. 99, No. 1, 2008, pp. 36–41.
59. Kilmametov, A., Ivanisenko, Y., Straumal, B., et al. “The α → ω Transformation in Titanium-Cobalt Alloys under High-Pressure Torsion,” *Metals*, V. 8, No. 1, 2017, p. 1.
60. Kilmametov, A. R., Ivanisenko, Yu., Mazilkin, A. A., et al. “The α→ω and β→ω phase transformations in Ti–Fe alloys under high-pressure torsion,” *Acta Materialia*, V. 144, 2018, pp. 337–51.
61. Kriegel, M. J., Kilmametov, A., Rudolph, M., et al. “Transformation Pathway upon Heating of Ti-Fe Alloys Deformed by High-Pressure Torsion,” *Advanced Engineering Materials*, V. 20, No. 4, 2018, p. 1700933.
62. Tane, M., Okuda, Y., Todaka, Y., et al. “Elastic properties of single-crystalline ω phase in titanium,” *Acta Materialia*, V. 61, No. 20, 2013, pp. 7543–54.
63. Panigrahi, A., Bönisch, M., Waitz, T., et al. “Thermal stability of hpt-induced omega phase in biocompatible Ti-16.1Nb alloys.” Proceedings of the International Conference on Solid-Solid Phase Transformations in Inorganic Materials 2015. 2015. p. 7.
64. Straumal, B. B., Kilmametov, A. R., Ivanisenko, Yu., et al. “Diffusive and displacive phase transitions in Ti–Fe and Ti–Co alloys under high pressure torsion,” *Journal of Alloys and Compounds*, V. 735, 2018, pp. 2281–6.
65. Edalati, K., and Horita, Z. “Phase transformations during high-pressure torsion (HPT) in titanium, cobalt and graphite,” *IOP Conference Series: Materials Science and Engineering*, V. 63, 2014, p. 012099.
66. Dey, G. K., Tewari, R., Banerjee, S., et al. “Formation of a shock deformation induced ω phase in Zr 20 Nb alloy,” *Acta Materialia*, V. 52, No. 18, 2004, pp. 5243–54.
67. Wood, R. M. “Martensitic alpha and omega phases as deformation products in a titanium-15% molybdenum alloy,” *Acta Metallurgica*, V. 11, 1963, pp. 907–14.
68. de Fontaine, D., Paton, N. E., and Williams, J. C. “The omega phase transformation in titanium alloys as an example of displacement controlled reactions,” *Acta Metallurgica*, V. 19, No. 11, 1971, pp. 1153–62.
69. Jones, N. G., Dashwood, R. J., Jackson, M., et al. “β Phase decomposition in Ti–5Al–5Mo–5V–3Cr,” *Acta Materialia*, V. 57, No. 13, 2009, pp. 3830–9.

70. Choudhuri, D., Zheng, Y., Alam, T., et al. “Coupled experimental and computational investigation of omega phase evolution in a high misfit titanium-vanadium alloy,” *Acta Materialia*, V. 130, 2017, pp. 215–28.
71. Ng, H. P., Devaraj, A., Nag, S., et al. “Phase separation and formation of omega phase in the beta matrix of a Ti–V–Cu alloy,” *Acta Materialia*, V. 59, No. 8, 2011, pp. 2981–91.
72. Zheng, Y., Banerjee, D., and Fraser, H. L. “A nano-scale instability in the β phase of dilute Ti–Mo alloys,” *Scripta Materialia*, V. 116, 2016, pp. 131–4.
73. Sukedai, E., and Matsumoto, H. “Annihilation behaviour under electron irradiation of athermal ω-phase crystals formed by cooling at 131K in a β-Ti-Mo alloy,” *Journal of Physics: Conference Series*, V. 241, 2010, p. 012106.
74. Coakley, J., Vorontsov, V. A., Littrell, K. C., et al. “Nanoprecipitation in a beta-titanium alloy,” *Journal of Alloys and Compounds*, V. 623, 2015, pp. 146–56.
75. Sukedai, E., Matsumoto, H., and Hashimoto, H. “Electron microscopy study on Mo content dependence of β to ω phase transformation due to cooling in Ti-Mo alloys,” *Journal of Electron Microscopy*, V. 51, 2002, pp. S143–7.
76. Hida, M., Sukedai, E., and Terauchi, H. “Microscopic approaches to isothermal transformation of incommensurate omega phase zones in Ti-20wt%Mo alloy studied by XDS, HREM and EXAFS,” *Acta Metallurgica*, V. 36, No. 6, 1988, pp. 1429–41.
77. Pynn, R. “The structure of the diffuse omega phase observed in Zr and Ti alloys,” *Journal of Physics F: Metal Physics*, V. 8, No. 1, 1978, pp. 1–13.
78. Li, M., and Min, X. “Origin of ω-phase formation in metastable β-type Ti-Mo alloys: cluster structure and stacking fault,” *Scientific Reports*, V. 10, No. 1, 2020, p. 8664.
79. de Fontaine, D. “Simple models for the omega phase transformation,” *Metallurgical Transactions A*, V. 19, No. 2, 1988, pp. 169–75.
80. Li, T., Kent, D., Sha, G., et al. “The role of ω in the precipitation of α in near-β Ti alloys,” *Scripta Materialia*, V. 117, 2016, pp. 92–5.
81. Kubo, H., and Farjami, S. “Lattice study of the incommensurate ω phase transition in Zr-Nb alloys,” *Physical Review B*, V. 83, No. 13, 2011, p. 134302.
82. Coakley, J., Vorontsov, V. A., Jones, N. G., et al. “Precipitation processes in the Beta-Titanium alloy Ti–5Al–5Mo–5V–3Cr,” *Journal of Alloys and Compounds*, V. 646, 2015, pp. 946–53.
83. Lai, M. J., Li, T., and Raabe, D. “ω phase acts as a switch between dislocation channeling and joint twinning- and transformation-induced plasticity in a metastable β titanium alloy,” *Acta Materialia*, V. 151, 2018, pp. 67–77.
84. Guo, S., Meng, Q.-K., Li, H.-P., et al. “Direct evidence for competition between metastable ω and equilibrium α phases in aged β-type Ti alloys,” *Rare Metals*, V. 33, No. 4, 2014, pp. 390–3.
85. Azimzadeh, S., and Rack, H. J. “Phase transformations in Ti-6.8Mo-4.5Fe-1.5Al,” *Metallurgical and Materials Transactions A*, V. 29, No. 10, 1998, pp. 2455–67.
86. Gloriant, T., Texier, G., Sun, F., et al. “Characterization of nanophase precipitation in a metastable β titanium-based alloy by electrical resistivity, dilatometry and neutron diffraction,” *Scripta Materialia*, V. 58, No. 4, 2008, pp. 271–4.
87. Coakley, J., Radecka, A., Dye, D., et al. “Characterizing nanoscale precipitation in a titanium alloy by laser-assisted atom probe tomography,” *Materials Characterization*, V. 141, 2018, pp. 129–38.
88. Li, C.-L., Mi, X.-J., Ye, W.-J., et al. “Influence of heat treatment on microstructure and tensile property of a new high strength beta alloy Ti–2Al–9.2Mo–2Fe,” *Materials Science and Engineering: A*, V. 580, 2013, pp. 250–6.
89. Min, X. H., Emura, S., Zhang, L., et al. “Effect of Fe and Zr additions on ω phase formation in β-type Ti–Mo alloys,” *Materials Science and Engineering: A*, V. 497, Nos. 1–2, 2008, pp. 74–8.

90. Prima, F., Debuigne, J., Boliveau, M., et al. “Control of omega phase volume fraction precipitated in a beta titanium alloy: Development of an experimental method,” *Journal of Materials Science Letters*, V. 19, 2000, pp. 2219–21.
91. Li, Q., Li, J., Ma, G., et al. “Influence of ω phase precipitation on mechanical performance and corrosion resistance of Ti–Nb–Zr alloy,” *Materials & Design*, V. 111, 2016, pp. 421–8.
92. Devaraj, A., Perea, D. E., Liu, J., et al. “Three-dimensional nanoscale characterisation of materials by atom probe tomography,” *International Materials Reviews*, V. 63, No. 2, 2018, pp. 68–101.
93. Devaraj, A., Williams, R. E. A., Nag, S., et al. “Three-dimensional morphology and composition of omega precipitates in a binary titanium–molybdenum alloy,” *Scripta Materialia*, V. 61, No. 7, 2009, pp. 701–4.
94. Niinomi, M., Nakai, M., Hendrickson, M., et al. “Influence of oxygen on omega phase stability in the Ti-29Nb-13Ta-4.6Zr alloy,” *Scripta Materialia*, V. 123, 2016, pp. 144–8.
95. Zheng, Y., Alam, T., Banerjee, R., et al. “The influence of aluminum and oxygen additions on intrinsic structural instabilities in titanium-molybdenum alloys,” *Scripta Materialia*, V. 152, 2018, pp. 150–3.
96. Moffat, D. L., and Larbalestier, D. C. “The competition between the alpha and omega phases in aged Ti-Nb alloys,” *Metallurgical Transactions A*, V. 19, No. 7, 1988, pp. 1687–94.
97. Hsu, H.-C., Wu, S.-C., Hsu, S.-K., et al. “Effects of chromium addition on structure and mechanical properties of Ti–5Mo alloy,” *Materials & Design (1980-2015)*, V. 65, 2015, pp. 700–6.
98. Tsuchiya, K., Emura, S., Ji, X., et al. “Plastic deformation of beta-Ti-Mo alloys with isothermal omega phase,” *MATEC Web of Conferences*, V. 321, 2020, p. 11087.
99. Hickman, B. S. “Omega phase precipitation in alloys of titanium with transition metals,” *Transactions of the Metallurgical Society of AIME*, V. 245, 1969, pp. 1329–36.
100. Prima, F., Vermaut, P., Gloriant, T., et al. “Experimental evidence of elastic interaction between ω nanoparticles embedded in a metastable β titanium alloy,” *Journal of Materials Science Letters*, V. 21, 2002, pp. 1935–7.
101. Williams, J. C., Hickman, B. S., and Leslie, D. H. “The Effect of Ternary Additions on the Decomposition of Metastable Beta-Phase Titanium Alloys,” *Metallurgical Transactions*, V. 2, 1971, pp. 477–84.
102. Hamajima, T., Luetjering, G., and Weissman, S. “Microstructure and Phase Relations for Ti-Mo-Al Alloys,” *Metallurgical Transactions*, V. 3, 1972, pp. 2805–10.
103. Froes, F. H., Yolton, C. F., Capenos, J. M., et al. “The Relationship Between Microstructure and Age Hardening Response in the Metastable Beta Titanium Alloy Ti-11.5 Mo-6 Zr-4.5 Sn (Beta III),” *Metallurgical Transactions A*, V. 11A, 1980, pp. 21–31.
104. Kent, D., Wang, G., Wang, W., et al. “Influence of ageing temperature and heating rate on the properties and microstructure of b-Ti alloy, Ti-6Cr-5Mo-5V-4Al,” *Materials Science and Engineering A*, V. 531, 2012, pp. 98–106.
105. Barriobero-Vila, P., Requena, G., Warchomicka, F., et al. “Phase transformation kinetics during continuous heating of a β-quenched Ti-10V-2Fe-3Al alloy,” *Journal of Materials Science*, V. 50, No. 3, 2015, pp. 1412–26.
106. Sun, F., Zhang, J. Y., Vermaut, P., et al. “Strengthening strategy for a ductile metastable β-titanium alloy using low-temperature aging,” *Materials Research Letters*, V. 5, No. 8, 2017, pp. 547–53.
107. Chen, J., Xiao, W., Dargusch, M. S., et al. “The Dependence of Isothermal ω Precipitation on the Quenching Rate in a Metastable β-Ti Alloy,” *Scientific Reports*, V. 5, No. 1, 2015, p. 14632.
108. Gullberg, R. B., Taggart, R., and Polonis, D. H. “On the decomposition of the beta phase in titanium alloys,” *Journal of Materials Science*, V. 6, 1971, pp. 384–9.
109. McCabe, K. K., and Sass, S. L. “The initial stages of the omega phase transformation in Ti-V alloys,” *Philosophical Magazine*, V. 23, No. 184, 1971, pp. 957–70.

110. Nag, S., Banerjee, R., and Fraser, H. L. “Intra-granular alpha precipitation in Ti–Nb–Zr–Ta biomedical alloys,” *Journal of Materials Science*, V. 44, No. 3, 2009, pp. 808–15.
111. Tane, M., Nishiyama, H., Umeda, A., et al. “Diffusionless isothermal omega transformation in titanium alloys driven by quenched-in compositional fluctuations,” *Physical Review Materials*, V. 3, No. 4, 2019, p. 043604.
112. Mantri, S. A., Choudhuri, D., Alam, T., et al. “Change in the deformation mode resulting from beta-omega compositional partitioning in a Ti Mo alloy: Room versus elevated temperature,” *Scripta Materialia*, V. 130, 2017, pp. 69–73.
113. Zheng, Y., Sosa, J. M., and Fraser, H. L. “On the influence of Athermal ω and a Phase Instabilities on the Scale of Precipitation of the α Phase in Metastable β-Ti Alloys,” *JOM*, V. 68, No. 5, 2016, pp. 1343–9.
114. Zheng, Y., Williams, R. E. A., Sosa, J. M., et al. “The role of the ω phase on the non-classical precipitation of the α phase in metastable β-titanium alloys,” *Scripta Materialia*, V. 111, 2016, pp. 81–4.
115. Furuhara, T., Maki, T., and Makino, T. “Microstructure control by thermomechanical processing in b-Ti±15±3 alloy,” *Journal of Materials Processing Technology*, 2001, p. 6.
116. Shi, R., Zheng, Y., Banerjee, R., et al. “ω-Assisted α nucleation in a metastable β titanium alloy,” *Scripta Materialia*, V. 171, 2019, pp. 62–6.
117. Niu, J. G., Ping, D. H., Ohno, T., et al. “Suppression effect of oxygen on the *β* to *ω* transformation in a *β* -type Ti alloy: insights from first-principles,” *Modelling and Simulation in Materials Science and Engineering*, V. 22, No. 1, 2014, p. 015007.
118. Coakley, J., Radecka, A., Dye, D., et al. “Isothermal omega formation and evolution in the Beta-Ti alloy Ti-5Al-5Mo-5V-3Cr,” *Philosophical Magazine Letters*, V. 96, No. 11, 2016, pp. 416–24.
119. Li, T., Ahmed, M., Sha, G., et al. “The influence of partitioning on the growth of intragranular α in near-β Ti alloys,” *Journal of Alloys and Compounds*, V. 643, 2015, pp. 212–22.
120. Wang, H. L., Hao, Y. L., He, S. Y., et al. “Elastically confined martensitic transformation at the nano-scale in a multifunctional titanium alloy,” *Acta Materialia*, V. 135, 2017, pp. 330–9.
121. Wang, H. L., Hao, Y. L., He, S. Y., et al. “Tracing the coupled atomic shear and shuffle for a cubic to a hexagonal crystal transition,” *Scripta Materialia*, V. 133, 2017, pp. 70–4.
122. Wang, H. L., Shah, S. A. A., Hao, Y. L., et al. “Stabilizing the body centered cubic crystal in titanium alloys by a nano-scale concentration modulation,” *Journal of Alloys and Compounds*, V. 700, 2017, pp. 155–8.
123. Hao, Y. L., Gong, D. L., Li, T., et al. “Continuous and reversible atomic rearrangement in a multifunctional titanium alloy,” *Materialia*, V. 2, 2018, pp. 1–8.
124. Li, T., Kent, D., Sha, G., et al. “Precipitation of the α-phase in an ultrafine grained beta-titanium alloy processed by severe plastic deformation,” *Materials Science and Engineering: A*, V. 605, 2014, pp. 144–50.
125. Wang, W., Zhang, X., Mei, W., et al. “Role of omega phase evolution in plastic deformation of twinning-induced plasticity β Ti–12V–2Fe–1Al alloy,” *Materials & Design*, V. 186, 2020, p. 108282.
126. Trinkle, D. R., Jones, M. D., Hennig, R. G., et al. “Empirical tight-binding model for titanium phase transformations,” *Physical Review B*, V. 73, No. 9, 2006, p. 094123.
127. Petry, W., Heiming, A., Trampenau, J., et al. “Phonon dispersion of the bcc phase of group-IV metals. I. bcc titanium,” *Physical Review B*, V. 43, No. 13, 1991, pp. 10933–47.
128. Hsu, H.-C., Wu, S.-C., Hsu, S.-K., et al. “Effects of heat treatments on the structure and mechanical properties of Zr–30Ti alloys,” *Materials Characterization*, V. 62, No. 2, 2011, pp. 157–63.
129. Ho, W.-F., Pan, C.-H., Wu, S.-C., et al. “Mechanical properties and deformation behavior of Ti–5Cr–xFe alloys,” *Journal of Alloys and Compounds*, V. 472, Nos. 1–2, 2009, pp. 546–50.

130. Ho, W.-F. “Effect of omega phase on mechanical properties of Ti-Mo alloys for biomedical applications,” *Journal of Medical and Biological Engineering*, V. 28, No. 1, 2008, pp. 47–51.
131. Coakley, J., Rahman, K. M., Vorontsov, V. A., et al. “Effect of precipitation on mechanical properties in the β-Ti alloy Ti–24Nb–4Zr–8Sn,” *Materials Science and Engineering: A*, V. 655, 2016, pp. 399–407.
132. Lasalmonie, A., and Loubradou, M. “The age hardening effect in Ti-6 Al-4 V due to ω and α precipitation in the β grains,” *Journal of Materials Science*, V. 14, 1979, pp. 2589–95.
133. Nakai, M., Niinomi, M., and Oneda, T. “Improvement in Fatigue Strength of Biomedical β-type Ti–Nb–Ta–Zr Alloy While Maintaining Low Young’s Modulus Through Optimizing ω-Phase Precipitation,” *Metallurgical and Materials Transactions A*, V. 43, No. 1, 2012, pp. 294–302.
134. Ng, H. P., Douguet, E., Bettles, C. J., et al. “Age-hardening behaviour of two metastable beta-titanium alloys,” *Materials Science and Engineering A*, V. 527, 2010, pp. 7017–26.
135. Chandrasekaran, V., Taggart, R., and Polonis, D. H. “Fracture Modes in a Binary Titanium Alloy,” *Metallography*, V. 5, 1972, pp. 235–50.
136. Feeney, J. A., and Blackburn, M. J. “Effect of Microstructure on the Strength, Toughness, and Stress-Corrosion Cracking Susceptibility of a Metastable Beta Titanium Alloy (Ti-11.5Mo-6Zr-4.5Sn),” *Metallurgical Transactions*, V. 1, 1970, pp. 3309–23.
137. Williams, J. C., Hickman, B. S., and Marcus, H. L. “The effect of omega phase on the mechanical properties of titanium alloys,” *Metallurgical Transactions*, V. 2, 1971, pp. 1913–9.
138. Wang, C. H., Yang, C. D., Liu, M., et al. “Martensitic microstructures and mechanical properties of as-quenched metastable β-type Ti–Mo alloys,” *Journal of Materials Science*, V. 51, No. 14, 2016, pp. 6886–96.
139. Terlinde, G. T., Duerig, T. W., and Williams, J. C. “Microstructure, tensile deformation, and fracture in aged ti 10V-2Fe-3Al,” *Metallurgical Transactions A*, V. 14, No. 10, 1983, pp. 2101–15.
140. Lilensten, L., Danard, Y., Brozek, C., et al. “On the heterogeneous nature of deformation in a strain-transformable beta metastable Ti-V-Cr-Al alloy,” *Acta Materialia*, V. 162, 2019, pp. 268–76.
141. Duerig, T. W., Allison, J. E., and Williams, J. C. “Microstructural influences on fatigue crack propagation in Ti-10V-2Fe-3Al,” *Metallurgical Transactions A*, V. 16, No. 5, 1985, pp. 739–51.
142. Zafari, A., Ding, Y., Cui, J., et al. “Achieving Fine Beta Grain Structure in a Metastable Beta Titanium Alloy Through Multiple Forging-Annealing Cycles,” *Metallurgical and Materials Transactions A*, V. 47, No. 7, 2016, pp. 3633–48.
143. Sadeghpour, S., Abbasi, S. M., Morakabati, M., et al. “Correlation between alpha phase morphology and tensile properties of a new beta titanium alloy,” *Materials & Design*, V. 121, 2017, pp. 24–35.